

Precision Studies and Searches for CP Asymmetries in the Inclusive Decay $\Lambda_c^+ \rightarrow \Lambda X$

M. Ablikim¹, M. N. Achasov^{4,c}, P. Adlarson⁸¹, X. C. Ai⁸⁷, C. S. Akondi^{31A,31B}, R. Aliberti³⁹, A. Amoroso^{80A,80C}, Q. An^{77,64,†}, Y. H. An⁸⁷, Y. Bai⁶², O. Bakina⁴⁰, Y. Ban^{50,h}, H.-R. Bao⁷⁰, X. L. Bao⁴⁹, V. Batozskaya^{1,48}, K. Begzsuren³⁵, N. Berger³⁹, M. Berlowski⁴⁸, M. B. Bertani^{30A}, D. Bettoni^{31A}, F. Bianchi^{80A,80C}, E. Bianco^{80A,80C}, A. Bortone^{80A,80C}, I. Boyko⁴⁰, R. A. Briere⁵, A. Brueggemann⁷⁴, H. Cai⁸², M. H. Cai^{42,k,l}, X. Cai^{1,64}, A. Calcaterra^{30A}, G. F. Cao^{1,70}, N. Cao^{1,70}, S. A. Cetin^{68A}, X. Y. Chai^{50,h}, J. F. Chang^{1,64}, T. T. Chang⁴⁷, G. R. Che⁴⁷, Y. Z. Che^{1,64,70}, C. H. Chen¹⁰, Chao Chen¹, G. Chen¹, H. S. Chen^{1,70}, H. Y. Chen²¹, M. L. Chen^{1,64,70}, S. J. Chen⁴⁶, S. M. Chen⁶⁷, T. Chen^{1,70}, W. Chen⁴⁹, X. R. Chen^{34,70}, X. T. Chen^{1,70}, X. Y. Chen^{12,g}, Y. B. Chen^{1,64}, Y. Q. Chen¹⁶, Z. K. Chen⁶⁵, J. Cheng⁴⁹, L. N. Cheng⁴⁷, S. K. Choi¹¹, X. Chu^{12,g}, G. Cibinetto^{31A}, F. Cossio^{80C}, J. Cottee-Meldrum⁶⁹, H. L. Dai^{1,64}, J. P. Dai⁸⁵, X. C. Dai⁶⁷, A. D. Dbeysi¹⁹, R. E. de Boer³, D. Dedovich⁴⁰, C. Q. Deng⁷⁸, Z. Y. Deng¹, A. Denig³⁹, I. Denisenko⁴⁰, M. Destefanis^{80A,80C}, F. De Mori^{80A,80C}, X. X. Ding^{50,h}, Y. Ding⁴⁴, Y. X. Ding³², J. Dong^{1,64}, L. Y. Dong^{1,70}, M. Y. Dong^{1,64,70}, X. Dong⁸², M. C. Du¹, S. X. Du⁸⁷, S. X. Du^{12,g}, X. L. Du^{12,g}, Y. Q. Du⁸², Y. Y. Duan⁶⁰, Z. H. Duan⁴⁶, P. Egorov^{40,b}, G. F. Fan⁴⁶, J. J. Fan²⁰, Y. H. Fan⁴⁹, J. Fang^{1,64}, J. Fang⁶⁵, S. S. Fang^{1,70}, W. X. Fang¹, Y. Q. Fang^{1,64,†}, L. Fava^{80B,80C}, F. Feldbauer³, G. Felici^{30A}, C. Q. Feng^{77,64}, J. H. Feng¹⁶, L. Feng^{42,k,l}, Q. X. Feng^{42,k,l}, Y. T. Feng^{77,64}, M. Fritsch³, C. D. Fu¹, J. L. Fu⁷⁰, Y. W. Fu^{1,70}, H. Gao⁷⁰, Y. Gao^{77,64}, Y. N. Gao^{50,h}, Y. N. Gao²⁰, Y. Y. Gao³², Z. Gao⁴⁷, S. Garbolino^{80C}, I. Garzia^{31A,31B}, L. Ge⁶², P. T. Ge²⁰, Z. W. Ge⁴⁶, C. Geng⁶⁵, E. M. Gersabeck⁷³, A. Gilman⁷⁵, K. Goetzen¹³, J. Gollub³, J. B. Gong^{1,70}, J. D. Gong³⁸, L. Gong⁴⁴, W. X. Gong^{1,64}, W. Gradl³⁹, S. Gramigna^{31A,31B}, M. Greco^{80A,80C}, M. D. Gu⁵⁵, M. H. Gu^{1,64}, C. Y. Guan^{1,70}, A. Q. Guo³⁴, J. N. Guo^{12,g}, L. B. Guo⁴⁵, M. J. Guo⁵⁴, R. P. Guo⁵³, X. Guo⁵⁴, Y. P. Guo^{12,g}, Z. Guo^{77,64}, A. Guskov^{40,b}, J. Gutierrez²⁹, J. Y. Han^{77,64}, T. T. Han¹, X. Han^{77,64}, F. Hanisch³, K. D. Hao^{77,64}, X. Q. Hao²⁰, F. A. Harris⁷¹, C. Z. He^{50,h}, K. K. He⁶⁰, K. L. He^{1,70}, F. H. Heinsius³, C. H. Heinz³⁹, Y. K. Heng^{1,64,70}, C. Herold¹⁶⁶, P. C. Hong³⁸, G. Y. Hou^{1,70}, X. T. Hou^{1,70}, Y. R. Hou⁷⁰, Z. L. Hou¹, H. M. Hu^{1,70}, J. F. Hu^{61,j}, Q. P. Hu^{77,64}, S. L. Hu^{12,g}, T. Hu^{1,64,70}, Y. Hu¹, Y. X. Hu⁸², Z. M. Hu⁶⁵, G. S. Huang^{77,64}, K. X. Huang⁶⁵, L. Q. Huang^{34,70}, P. Huang⁶⁷, X. T. Huang⁵⁴, Y. P. Huang¹, Y. S. Huang⁶⁵, T. Hussain⁷⁹, N. Hüskens³⁹, N. in der Wiesche⁷⁴, J. Jackson²⁹, Q. Ji¹, Q. P. Ji²⁰, W. Ji^{1,70}, X. B. Ji^{1,70}, X. L. Ji^{1,64}, L. K. Jia⁷⁰, X. Q. Jia⁵⁴, Z. K. Jia^{77,64}, D. Jiang^{1,70}, H. B. Jiang⁸², P. C. Jiang^{50,h}, S. J. Jiang¹⁰, X. S. Jiang^{1,64,70}, Y. Jiang⁷⁰, J. B. Jiao⁵⁴, J. K. Jiao³⁸, Z. Jiao²⁵, L. C. L. Jin¹, S. Jin⁴⁶, Y. Jin⁷², M. Q. Jing^{1,70}, X. M. Jing⁷⁰, T. Johansson⁸¹, S. Kabana³⁶, X. L. Kang¹⁰, X. S. Kang⁴⁴, B. C. Ke⁸⁷, V. Khachatryan²⁹, A. Khoukaz⁷⁴, O. B. Kolcu^{68A}, B. Kopf³, L. Kröger⁷⁴, L. Krümmel³, Y. Y. Kuang⁷⁸, M. Kuessner³, X. Kui^{1,70}, N. Kumar²⁸, A. Kupsc^{48,81}, W. Kühn⁴¹, Q. Lan⁷⁸, W. N. Lan²⁰, T. T. Lei^{77,64}, M. Lellmann³⁹, T. Lenz³⁹, C. Li⁵¹, C. Li⁴⁷, C. H. Li⁴⁵, C. K. Li²¹, C. K. Li⁴⁷, D. M. Li⁸⁷, F. Li^{1,64}, G. Li¹, H. B. Li^{1,70}, H. J. Li²⁰, H. L. Li⁸⁷, H. N. Li^{61,j}, H. P. Li⁴⁷, Hui Li⁴⁷, J. S. Li⁶⁵, J. W. Li⁵⁴, K. Li¹, K. L. Li^{42,k,l}, L. J. Li^{1,70}, Lei Li⁵², M. H. Li⁴⁷, M. R. Li^{1,70}, P. L. Li⁷⁰, P. R. Li^{42,k,l}, Q. M. Li^{1,70}, Q. X. Li⁵⁴, R. Li^{18,34}, S. Li⁸⁷, S. X. Li¹², S. Y. Li⁸⁷, Shanshan Li^{27,i}, T. Li⁵⁴, T. Y. Li⁴⁷, W. D. Li^{1,70}, W. G. Li^{1,†}, X. Li^{1,70}, X. H. Li^{77,64}, X. K. Li^{50,h}, X. L. Li⁵⁴, X. Y. Li^{1,9}, X. Z. Li⁶⁵, Y. Li²⁰, Y. G. Li⁷⁰, Y. P. Li³⁸, Z. H. Li⁴², Z. J. Li⁶⁵, Z. L. Li⁸⁷, Z. X. Li⁴⁷, Z. Y. Li⁸⁵, C. Liang⁴⁶, H. Liang^{77,64}, Y. F. Liang⁵⁹, Y. T. Liang^{34,70}, G. R. Liao¹⁴, L. B. Liao⁶⁵, M. H. Liao⁶⁵, Y. P. Liao^{1,70}, J. Libby²⁸, A. Limphirat⁶⁶, C. C. Lin⁶⁰, D. X. Lin^{34,70}, T. Lin¹, B. J. Liu¹, B. X. Liu⁸², C. Liu³⁸, C. X. Liu¹, F. H. Liu⁵⁸, Feng Liu⁶, G. M. Liu^{61,j}, H. H. Liu^{42,k,l}, H. B. Liu¹⁵, H. M. Liu^{1,70}, Huihui Liu²², J. B. Liu^{77,64}, J. J. Liu²¹, K. Liu^{42,k,l}, K. Liu⁷⁸, K. Y. Liu⁴⁴, Ke Liu²³, L. Liu⁴², L. C. Liu⁴⁷, Lu Liu⁴⁷, M. H. Liu³⁸, P. L. Liu⁵⁴, Q. Liu⁷⁰, S. B. Liu^{77,64}, T. Liu¹, W. M. Liu^{77,64}, W. T. Liu⁴³, X. Liu^{42,k,l}, X. K. Liu^{42,k,l}, X. L. Liu^{12,g}, X. P. Liu^{12,g}, X. Y. Liu⁸², Y. Liu^{42,k,l}, Y. Liu⁸⁷, Y. B. Liu⁴⁷, Z. A. Liu^{1,64,70}, Z. D. Liu⁸³, Z. L. Liu⁷⁸, Z. Q. Liu⁵⁴, Z. Y. Liu⁴², X. C. Lou^{1,64,70}, H. J. Lu²⁵, J. G. Lu^{1,64}, X. L. Lu¹⁶, Y. Lu⁷, Y. H. Lu^{1,70}, Y. P. Lu^{1,64}, Z. H. Lu^{1,70}, C. L. Luo⁴⁵, J. R. Luo⁶⁵, J. S. Luo^{1,70}, M. X. Luo⁸⁶, T. Luo^{12,g}, X. L. Luo^{1,64}, Z. Y. Lv²³, X. R. Lyu^{70,o}, Y. F. Lyu⁴⁷, Y. H. Lyu⁸⁷, F. C. Ma⁴⁴, H. L. Ma¹, Heng Ma^{27,i}, J. L. Ma^{1,70}, L. L. Ma⁵⁴, L. R. Ma⁷², Q. M. Ma¹, R. Q. Ma^{1,70}, R. Y. Ma²⁰, T. Ma^{77,64}, X. T. Ma^{1,70}, X. Y. Ma^{1,64}, Y. M. Ma³⁴, F. E. Maas¹⁹, I. MacKay⁷⁵, M. Maggiora^{80A,80C}, S. Malde⁷⁵, Q. A. Malik⁷⁹, H. X. Mao^{42,k,l}, Y. J. Mao^{50,h}, Z. P. Mao¹, S. Marcello^{80A,80C}, A. Marshall⁶⁹, F. M. Melendi^{31A,31B}, Y. H. Meng⁷⁰, Z. X. Meng⁷², G. Mezzadri^{31A}, H. Miao^{1,70}, T. J. Min⁴⁶, R. E. Mitchell²⁹, X. H. Mo^{1,64,70}, B. Moses²⁹, N. Yu. Muchnoi^{4,c}, J. Muskalla³⁹, Y. Nefedov⁴⁰, F. Nerling^{19,e}, H. Neuwirth⁷⁴, Z. Ning^{1,64}, S. Nisar^{33,a}, Q. L. Niu^{42,k,l}, W. D. Niu^{12,g}, Y. Niu⁵⁴, C. Normand⁶⁹, S. L. Olsen^{11,70}, Q. Ouyang^{1,64,70}, S. Pacetti^{30B,30C}, X. Pan⁶⁰, Y. Pan⁶², A. Pathak¹¹, Y. P. Pei^{77,64}, M. Pelizaeus³, G. L. Peng^{77,64}, H. P. Peng^{77,64}, X. J. Peng^{42,k,l}, Y. Y. Peng^{42,k,l}, K. Peters^{13,e}, K. Petridis⁶⁹, J. L. Ping⁴⁵, R. G. Ping^{1,70}, S. Plura³⁹, V. Prasad³⁸, F. Z. Qi¹, H. R. Qi⁶⁷, M. Qi⁴⁶, S. Qian^{1,64}, W. B. Qian⁷⁰, C. F. Qiao⁷⁰, J. H. Qiao²⁰, J. J. Qin⁷⁸, J. L. Qin⁶⁰, L. Q. Qin¹⁴, L. Y. Qin^{77,64}, P. B. Qin⁷⁸, X. P. Qin⁴³, X. S. Qin⁵⁴, Z. H. Qin^{1,64}, J. F. Qiu¹, Z. H. Qu⁷⁸, J. Rademacker⁶⁹, C. F. Redmer³⁹, A. Rivetti^{80C}, M. Rolo^{80C}, G. Rong^{1,70}, S. S. Rong^{1,70}, F. Rosini^{30B,30C}, Ch. Rosner¹⁹, M. Q. Ruan^{1,64}, N. Salone^{48,p}, A. Sarantsev^{40,d}, Y. Schelhaas³⁹, K. Schoenning⁸¹, M. Scodeggio^{31A}, W. Shan²⁶, X. Y. Shan^{77,64}, Z. J. Shang^{42,k,l}, J. F. Shangguan¹⁷, L. G. Shao^{1,70}, M. Shao^{77,64}, C. P. Shen^{12,g}, H. F. Shen^{1,9}, W. H. Shen⁷⁰,

X. Y. Shen^{1,70} , B. A. Shi⁷⁰ , H. Shi^{77,64} , J. L. Shi^{8,q} , J. Y. Shi¹ , M. H. Shi⁸⁷ , S. Y. Shi⁷⁸ , X. Shi^{1,64} ,
H. L. Song^{77,64} , J. J. Song²⁰ , M. H. Song⁴² , T. Z. Song⁶⁵ , W. M. Song³⁸ , Y. X. Song^{50,h,m} , Zirong Song^{27,i} ,
S. Sosio^{80A,80C} , S. Spataro^{80A,80C} , S. Stansilau⁷⁵ , F. Stieler³⁹ , M. Stolte³ , S. S. Su⁴⁴ , G. B. Sun⁸² ,
G. X. Sun¹ , H. Sun⁷⁰ , H. K. Sun¹ , J. F. Sun²⁰ , K. Sun⁶⁷ , L. Sun⁸² , R. Sun⁷⁷ , S. S. Sun^{1,70} , T. Sun^{56,f} ,
W. Y. Sun⁵⁵ , Y. C. Sun⁸² , Y. H. Sun³² , Y. J. Sun^{77,64} , Y. Z. Sun¹ , Z. Q. Sun^{1,70} , Z. T. Sun⁵⁴ ,
C. J. Tang⁵⁹ , G. Y. Tang¹ , J. Tang⁶⁵ , J. J. Tang^{77,64} , L. F. Tang⁴³ , Y. A. Tang⁸² , L. Y. Tao⁷⁸ , M. Tai⁷⁵ ,
J. X. Teng^{77,64} , J. Y. Tian^{77,64} , W. H. Tian⁶⁵ , Y. Tian³⁴ , Z. F. Tian⁸² , I. Uman^{68B} , E. van der Smagt³ ,
B. Wang¹ , B. Wang⁶⁵ , Bo Wang^{77,64} , C. Wang^{42,k,l} , C. Wang²⁰ , Cong Wang²³ , D. Y. Wang^{50,h} ,
H. J. Wang^{42,k,l} , H. R. Wang⁸⁴ , J. Wang¹⁰ , J. J. Wang⁸² , J. P. Wang³⁷ , K. Wang^{1,64} , L. L. Wang¹ ,
L. W. Wang³⁸ , M. Wang⁵⁴ , M. Wang^{77,64} , N. Y. Wang⁷⁰ , S. Wang^{42,k,l} , Shun Wang⁶³ , T. Wang^{12,g} ,
T. J. Wang⁴⁷ , W. Wang⁶⁵ , W. P. Wang³⁹ , X. F. Wang^{42,k,l} , X. L. Wang^{12,g} , X. N. Wang^{1,70} , Xin Wang^{27,i} ,
Y. Wang¹ , Y. D. Wang⁴⁹ , Y. F. Wang^{1,9,70} , Y. H. Wang^{42,k,l} , Y. J. Wang^{77,64} , Y. L. Wang²⁰ , Y. N. Wang⁴⁹ ,
Y. N. Wang⁸² , Yaqian Wang¹⁸ , Yi Wang⁶⁷ , Yuan Wang^{18,34} , Z. Wang^{1,64} , Z. Wang⁴⁷ , Z. L. Wang² ,
Z. Q. Wang^{12,g} , Z. Y. Wang^{1,70} , Ziyi Wang⁷⁰ , D. Wei⁴⁷ , D. H. Wei¹⁴ , H. R. Wei⁴⁷ , F. Weidner⁷⁴ ,
S. P. Wen¹ , U. Wiedner³ , G. Wilkinson⁷⁵ , M. Wolke⁸¹ , J. F. Wu^{1,9} , L. H. Wu¹ , L. J. Wu²⁰ , Lianjie Wu²⁰ ,
S. G. Wu^{1,70} , S. M. Wu⁷⁰ , X. W. Wu⁷⁸ , Z. Wu^{1,64} , H. L. Xia^{77,64} , L. Xia^{77,64} , B. H. Xiang^{1,70} ,
D. Xiao^{42,k,l} , G. Y. Xiao⁴⁶ , H. Xiao⁷⁸ , Y. L. Xiao^{12,g} , Z. J. Xiao⁴⁵ , C. Xie⁴⁶ , K. J. Xie^{1,70} , Y. Xie⁵⁴ ,
Y. G. Xie^{1,64} , Y. H. Xie⁶ , Z. P. Xie^{77,64} , T. Y. Xing^{1,70} , D. B. Xiong¹ , C. J. Xu⁶⁵ , G. F. Xu¹ , H. Y. Xu² ,
M. Xu^{77,64} , Q. J. Xu¹⁷ , Q. N. Xu³² , T. D. Xu⁷⁸ , X. P. Xu⁶⁰ , Y. Xu^{12,g} , Y. C. Xu⁸⁴ , Z. S. Xu⁷⁰ ,
F. Yan²⁴ , L. Yan^{12,g} , W. B. Yan^{77,64} , W. C. Yan⁸⁷ , W. H. Yan⁶ , W. P. Yan²⁰ , X. Q. Yan^{12,g} , Y. Y. Yan⁶⁶ ,
H. J. Yang^{56,f} , H. L. Yang³⁸ , H. X. Yang¹ , J. H. Yang⁴⁶ , R. J. Yang²⁰ , Y. Yang^{12,g} , Y. H. Yang⁴⁶ ,
Y. H. Yang⁴⁷ , Y. M. Yang⁸⁷ , Y. Q. Yang¹⁰ , Y. Z. Yang²⁰ , Z. Y. Yang⁷⁸ , Z. P. Yao⁵⁴ , M. Ye^{1,64} ,
M. H. Ye^{9,†} , Z. J. Ye^{61,j} , Junhao Yin⁴⁷ , Z. Y. You⁶⁵ , B. X. Yu^{1,64,70} , C. X. Yu⁴⁷ , G. Yu¹³ , J. S. Yu^{27,i} ,
L. W. Yu^{12,g} , T. Yu⁷⁸ , X. D. Yu^{50,h} , Y. C. Yu⁸⁷ , Y. C. Yu⁴² , C. Z. Yuan^{1,70} , H. Yuan^{1,70} , J. Yuan³⁸ ,
J. Yuan⁴⁹ , L. Yuan² , M. K. Yuan^{12,g} , S. H. Yuan⁷⁸ , Y. L. Yuan^{1,70} , C. X. Yue⁴³ , Ying Yue²⁰ , A. A. Zafar⁷⁹ ,
F. R. Zeng⁵⁴ , S. H. Zeng⁶⁹ , X. Zeng^{12,g} , Yujie Zeng⁶⁵ , Y. J. Zeng^{1,70} , Y. C. Zhai⁵⁴ , Y. H. Zhan⁶⁵ ,
Shunan Zhang⁷⁵ , B. L. Zhang^{1,70} , B. X. Zhang^{1,†} , D. H. Zhang⁴⁷ , G. Y. Zhang²⁰ , G. Y. Zhang^{1,70} ,
H. Zhang^{77,64} , H. Zhang⁸⁷ , H. C. Zhang^{1,64,70} , H. H. Zhang⁶⁵ , H. Q. Zhang^{1,64,70} , H. R. Zhang^{77,64} ,
H. Y. Zhang^{1,64} , J. Zhang⁶⁵ , J. Zhang⁵² , J. J. Zhang⁵⁷ , J. L. Zhang²¹ , J. Q. Zhang⁴⁵ , J. S. Zhang^{12,g} ,
J. W. Zhang^{1,64,70} , J. X. Zhang^{42,k,l} , J. Y. Zhang¹ , J. Y. Zhang^{12,g} , J. Z. Zhang^{1,70} , Jianyu Zhang⁷⁰ ,
L. M. Zhang⁶⁷ , Lei Zhang⁴⁶ , N. Zhang³⁸ , P. Zhang^{1,9} , Q. Zhang²⁰ , Q. Y. Zhang³⁸ , Q. Z. Zhang⁷⁰ ,
R. Y. Zhang^{42,k,l} , S. H. Zhang^{1,70} , Shulei Zhang^{27,i} , X. M. Zhang¹ , X. Y. Zhang⁵⁴ , Y. Zhang¹ , Y. Zhang⁷⁸ ,
Y. T. Zhang⁸⁷ , Y. H. Zhang^{1,64} , Y. P. Zhang^{77,64} , Z. D. Zhang¹ , Z. H. Zhang¹ , Z. L. Zhang³⁸ ,
Z. L. Zhang⁶⁰ , Z. X. Zhang²⁰ , Z. Y. Zhang⁸² , Z. Y. Zhang⁴⁷ , Z. Y. Zhang⁴⁹ , Zh. Zh. Zhang²⁰ , G. Zhao¹ ,
J.-P. Zhao⁷⁰ , J. Y. Zhao^{1,70} , J. Z. Zhao^{1,64} , L. Zhao¹ , L. Zhao^{77,64} , M. G. Zhao⁴⁷ , R. P. Zhao⁷⁰ ,
S. J. Zhao⁸⁷ , Y. B. Zhao^{1,64} , Y. L. Zhao⁶⁰ , Y. P. Zhao⁴⁹ , Y. X. Zhao^{34,70} , Z. G. Zhao^{77,64} ,
A. Zhemchugov^{40,b} , B. Zheng⁷⁸ , B. M. Zheng³⁸ , J. P. Zheng^{1,64} , W. J. Zheng^{1,70} , W. Q. Zheng¹⁰ ,
X. R. Zheng²⁰ , Y. H. Zheng^{70,o} , B. Zhong⁴⁵ , C. Zhong²⁰ , H. Zhou^{39,54,n} , J. Q. Zhou³⁸ , S. Zhou⁶ ,
X. Zhou⁸² , X. K. Zhou⁶ , X. R. Zhou^{77,64} , X. Y. Zhou⁴³ , Y. X. Zhou⁸⁴ , Y. Z. Zhou^{12,g} , A. N. Zhu⁷⁰ ,
J. Zhu⁴⁷ , K. Zhu¹ , K. J. Zhu^{1,64,70}

- ²¹ Henan University, Kaifeng 475004, People's Republic of China
- ²² Henan University of Science and Technology, Luoyang 471003, People's Republic of China
- ²³ Henan University of Technology, Zhengzhou 450001, People's Republic of China
- ²⁴ Hengyang Normal University, Hengyang 421001, People's Republic of China
- ²⁵ Huangshan College, Huangshan 245000, People's Republic of China
- ²⁶ Hunan Normal University, Changsha 410081, People's Republic of China
- ²⁷ Hunan University, Changsha 410082, People's Republic of China
- ²⁸ Indian Institute of Technology Madras, Chennai 600036, India
- ²⁹ Indiana University, Bloomington, Indiana 47405, USA
- ³⁰ INFN Laboratori Nazionali di Frascati, (A)INFN Laboratori Nazionali di Frascati, I-00044, Frascati, Italy; (B)INFN Sezione di Perugia, I-06100, Perugia, Italy; (C)University of Perugia, I-06100, Perugia, Italy
- ³¹ INFN Sezione di Ferrara, (A)INFN Sezione di Ferrara, I-44122, Ferrara, Italy; (B)University of Ferrara, I-44122, Ferrara, Italy
- ³² Inner Mongolia University, Hohhot 010021, People's Republic of China
- ³³ Institute of Business Administration, Karachi,
- ³⁴ Institute of Modern Physics, Lanzhou 730000, People's Republic of China
- ³⁵ Institute of Physics and Technology, Mongolian Academy of Sciences, Peace Avenue 54B, Ulaanbaatar 13330, Mongolia
- ³⁶ Instituto de Alta Investigación, Universidad de Tarapacá, Casilla 7D, Arica 1000000, Chile
- ³⁷ Jiangsu Ocean University, Lianyungang 222000, People's Republic of China
- ³⁸ Jilin University, Changchun 130012, People's Republic of China
- ³⁹ Johannes Gutenberg University of Mainz, Johann-Joachim-Becher-Weg 45, D-55099 Mainz, Germany
- ⁴⁰ Joint Institute for Nuclear Research, 141980 Dubna, Moscow region, Russia
- ⁴¹ Justus-Liebig-Universität Giessen, II. Physikalisches Institut, Heinrich-Buff-Ring 16, D-35392 Giessen, Germany
- ⁴² Lanzhou University, Lanzhou 730000, People's Republic of China
- ⁴³ Liaoning Normal University, Dalian 116029, People's Republic of China
- ⁴⁴ Liaoning University, Shenyang 110036, People's Republic of China
- ⁴⁵ Nanjing Normal University, Nanjing 210023, People's Republic of China
- ⁴⁶ Nanjing University, Nanjing 210093, People's Republic of China
- ⁴⁷ Nankai University, Tianjin 300071, People's Republic of China
- ⁴⁸ National Centre for Nuclear Research, Warsaw 02-093, Poland
- ⁴⁹ North China Electric Power University, Beijing 102206, People's Republic of China
- ⁵⁰ Peking University, Beijing 100871, People's Republic of China
- ⁵¹ Qufu Normal University, Qufu 273165, People's Republic of China
- ⁵² Renmin University of China, Beijing 100872, People's Republic of China
- ⁵³ Shandong Normal University, Jinan 250014, People's Republic of China
- ⁵⁴ Shandong University, Jinan 250100, People's Republic of China
- ⁵⁵ Shandong University of Technology, Zibo 255000, People's Republic of China
- ⁵⁶ Shanghai Jiao Tong University, Shanghai 200240, People's Republic of China
- ⁵⁷ Shanxi Normal University, Linfen 041004, People's Republic of China
- ⁵⁸ Shanxi University, Taiyuan 030006, People's Republic of China
- ⁵⁹ Sichuan University, Chengdu 610064, People's Republic of China
- ⁶⁰ Soochow University, Suzhou 215006, People's Republic of China
- ⁶¹ South China Normal University, Guangzhou 510006, People's Republic of China
- ⁶² Southeast University, Nanjing 211100, People's Republic of China
- ⁶³ Southwest University of Science and Technology, Mianyang 621010, People's Republic of China
- ⁶⁴ State Key Laboratory of Particle Detection and Electronics, Beijing 100049, Hefei 230026, People's Republic of China
- ⁶⁵ Sun Yat-Sen University, Guangzhou 510275, People's Republic of China
- ⁶⁶ Suranaree University of Technology, University Avenue 111, Nakhon Ratchasima 30000, Thailand
- ⁶⁷ Tsinghua University, Beijing 100084, People's Republic of China
- ⁶⁸ Turkish Accelerator Center Particle Factory Group, (A)Istinye University, 34010, Istanbul, Turkey; (B)Near East University, Nicosia, North Cyprus, 99138, Mersin 10, Turkey
- ⁶⁹ University of Bristol, H H Wills Physics Laboratory, Tyndall Avenue, Bristol, BS8 1TL, UK
- ⁷⁰ University of Chinese Academy of Sciences, Beijing 100049, People's Republic of China
- ⁷¹ University of Hawaii, Honolulu, Hawaii 96822, USA
- ⁷² University of Jinan, Jinan 250022, People's Republic of China
- ⁷³ University of Manchester, Oxford Road, Manchester, M13 9PL, United Kingdom
- ⁷⁴ University of Muenster, Wilhelm-Klemm-Strasse 9, 48149 Muenster, Germany
- ⁷⁵ University of Oxford, Keble Road, Oxford OX13RH, United Kingdom
- ⁷⁶ University of Science and Technology Liaoning, Anshan 114051, People's Republic of China
- ⁷⁷ University of Science and Technology of China, Hefei 230026, People's Republic of China
- ⁷⁸ University of South China, Hengyang 421001, People's Republic of China
- ⁷⁹ University of the Punjab, Lahore-54590, Pakistan
- ⁸⁰ University of Turin and INFN, (A)University of Turin, I-10125, Turin, Italy; (B)University of Eastern Piedmont, I-15121, Alessandria, Italy; (C)INFN, I-10125, Turin, Italy

⁸¹ Uppsala University, Box 516, SE-75120 Uppsala, Sweden

⁸² Wuhan University, Wuhan 430072, People's Republic of China

⁸³ Xi'an Jiaotong University, No.28 Xianning West Road, Xi'an, Shaanxi 710049, P.R. China

⁸⁴ Yantai University, Yantai 264005, People's Republic of China

⁸⁵ Yunnan University, Kunming 650500, People's Republic of China

⁸⁶ Zhejiang University, Hangzhou 310027, People's Republic of China

⁸⁷ Zhengzhou University, Zhengzhou 450001, People's Republic of China

† Deceased

^a Also at Bogazici University, 34342 Istanbul, Turkey

^b Also at the Moscow Institute of Physics and Technology, Moscow 141700, Russia

^c Also at the Novosibirsk State University, Novosibirsk, 630090, Russia

^d Also at the NRC "Kurchatov Institute", PNPI, 188300, Gatchina, Russia

^e Also at Goethe University Frankfurt, 60323 Frankfurt am Main, Germany

^f Also at Key Laboratory for Particle Physics, Astrophysics and Cosmology, Ministry of Education; Shanghai Key Laboratory for Particle Physics and Cosmology; Institute of Nuclear and Particle Physics, Shanghai 200240, People's Republic of China

^g Also at Key Laboratory of Nuclear Physics and Ion-beam Application (MOE) and Institute of Modern Physics, Fudan University, Shanghai 200443, People's Republic of China

^h Also at State Key Laboratory of Nuclear Physics and Technology, Peking University, Beijing 100871, People's Republic of China

ⁱ Also at School of Physics and Electronics, Hunan University, Changsha 410082, China

^j Also at Guangdong Provincial Key Laboratory of Nuclear Science, Institute of Quantum Matter, South China Normal University, Guangzhou 510006, China

^k Also at MOE Frontiers Science Center for Rare Isotopes, Lanzhou University, Lanzhou 730000, People's Republic of China

^l Also at Lanzhou Center for Theoretical Physics, Lanzhou University, Lanzhou 730000, People's Republic of China

^m Also at Ecole Polytechnique Federale de Lausanne (EPFL), CH-1015 Lausanne, Switzerland

ⁿ Also at Helmholtz Institute Mainz, Staudinger Weg 18, D-55099 Mainz, Germany

^o Also at Hangzhou Institute for Advanced Study, University of Chinese Academy of Sciences, Hangzhou 310024, China

^p Currently at Silesian University in Katowice, Chorzow, 41-500, Poland

^q Also at Applied Nuclear Technology in Geosciences Key Laboratory of Sichuan Province, Chengdu University of Technology, Chengdu 610059, People's Republic of China

Based on e^+e^- annihilation data collected with the BESIII detector at center-of-mass energies from 4.600 to 4.699 GeV, corresponding to an integrated luminosity of 4.5 fb^{-1} , we present the first measurement of the longitudinal polarization of Λ hyperons produced in the inclusive decay $\Lambda_c^+ \rightarrow \Lambda X$, where X denotes any allowed final state. The polarizations are determined to be $\mathcal{P}_\Lambda = -0.393 \pm 0.055_{\text{sta.}} \pm 0.020_{\text{sys.}}$ and $\mathcal{P}_{\bar{\Lambda}} = 0.288 \pm 0.056_{\text{sta.}} \pm 0.017_{\text{sys.}}$. We then search for CP violation using an asymmetry constructed from the Λ polarization and the $\Lambda \rightarrow p\pi^-$ decay asymmetry parameters, and obtain $\mathcal{A}_{\text{CP}}^{\text{pol}} = 0.15 \pm 0.12_{\text{sta.}} \pm 0.04_{\text{sys.}}$. We also perform an updated measurement of the absolute branching fraction, resulted as $\mathcal{B}(\Lambda_c^+ \rightarrow \Lambda X) = (38.07 \pm 0.38_{\text{sta.}} \pm 0.49_{\text{sys.}})\%$, with precision improved by a factor of four relative to the current world average. A search for direct CP violation yields $\mathcal{A}_{\text{CP}}^{\text{dir}} = (1.5 \pm 1.0_{\text{sta.}} \pm 1.0_{\text{sys.}})\%$. No evidence for CP violation in inclusive charm baryon decays is observed.

The Standard Model (SM) is the most successful and well-tested theory in particle physics, offering a comprehensive framework to describe elementary particles and their fundamental interactions. However, it does not provide a quantitatively sufficient explanation of the observed matter-antimatter asymmetry of the Universe. In 1967, Sakharov proposed that the violation of charge conjugation (C) and charge-parity (CP) symmetry is one of the necessary conditions to explain the baryon asymmetry of the universe [1]. Over the decades, CP violation (CPV) has been extensively studied in meson systems, first observed in neutral K decays and later established in the B and D sectors [2–5]. However, the observable universe is dominated by baryon asymmetry, suggesting that CPV in the baryon sector may play a qualitatively different and potentially critical role. Recently, the LHCb Collaboration reported the first observation of CPV in

the b -baryon decay $\Lambda_b^0 \rightarrow pK^-\pi^+\pi^-$ [6], with the result consistent with SM predictions. In contrast, despite increasing statistics in various experiments, no evidence of CPV has been observed in the charm baryon sector. This is primarily because Standard Model predictions for charm CP asymmetries are suppressed to the order of $\mathcal{O}(10^{-4} - 10^{-3})$ [7], making such searches experimentally challenging.

As the lightest charm baryon, the Λ_c^+ serves as a cornerstone for studying weak decays, offering a unique window into the interplay of weak and strong interactions in the baryon sector [8, 9]. Compared to mesons, the three-quark structure of baryons leads to a richer phenomenology in decay dynamics [10]. Among all studies, inclusive measurements are particularly valuable as they constrain the total decay width and quantify contributions from unmeasured channels. Currently, the sum of

all measured exclusive decay modes of Λ_c^+ containing a Λ in final states accounts for only $(31.36 \pm 1.09)\%$ of the total width [11]. In contrast, the inclusive branching fraction (BF) of $\Lambda_c^+ \rightarrow \Lambda X$ was measured by BESIII to be $(38.2_{-2.2}^{+2.8} \pm 0.9)\%$, utilizing a data sample corresponding to 586.9 pb^{-1} [12]. This discrepancy highlights the existence of undiscovered decay modes, but with limited precision. Thus a more accurate inclusive BF measurement is necessary. Precise knowledge of $\mathcal{B}(\Lambda_c^+ \rightarrow \Lambda X)$ is not only important for understanding the charm baryon decay dynamics, but also provides essential input for modeling b -flavored hadron decays and testing heavy quark effective theory [13].

In addition to branching fraction, baryon polarization in weak decay provides a sensitive probe of parity-violating weak dynamics [8, 14]. Previous searches for CPV in charm baryons have focused on exclusive modes, such as $\Lambda_c^+ \rightarrow \Lambda K^+$ and $\Lambda_c^+ \rightarrow \Sigma^0 K^+$ [15, 16], with results indicating no CPV. While local asymmetries arising from interference in specific exclusive channels may cancel upon integration, a non-zero inclusive asymmetry would indicate a net, integrated difference in decay dynamics between baryons and anti-baryons. This motivates inclusive CPV searches as a complementary approach, with the practical advantages of larger signal yields and reduced reliance on modeling individual subchannels [17]. The inclusive decay $\Lambda_c^+ \rightarrow \Lambda X$ has been proposed as a probe of net CPV in the baryon sector [17], for which Standard Model effects are expected to be $\mathcal{O}(10^{-5} \sim 10^{-4})$.

In this Letter, the inclusive decay $\Lambda_c^+ \rightarrow \Lambda X$ is studied with a double tag (DT) method [18]. The $\bar{\Lambda}_c^-$ baryon is reconstructed in one of the eleven single tag (ST) modes ($\bar{p}K_S^0$, $\bar{p}K^+\pi^-$, $\bar{p}K_S^0\pi^0$, $\bar{p}K_S^0\pi^-\pi^+$, $\bar{p}K^+\pi^-\pi^0$, $\bar{\Lambda}\pi^-$, $\bar{\Lambda}\pi^-\pi^0$, $\bar{\Lambda}\pi^-\pi^+\pi^-$, $\bar{\Sigma}^0\pi^-$, $\bar{\Sigma}^-\pi^0$ and $\bar{\Sigma}^-\pi^-\pi^+$). Using e^+e^- annihilation data, corresponding to an integrated luminosity of 4.5 fb^{-1} , collected at center-of-mass energies between 4.600 and 4.699 GeV with the BESIII detector at BEPCII [19, 20], we investigate direct and polarization-dependent CPV in the inclusive decay $\Lambda_c^+ \rightarrow \Lambda X$, and report measurements of its BF and the longitudinal polarization of Λ hyperon produced in this decay. These results offer new insights to improve our understanding of CPV in charm baryons and the properties of inclusive decays. Charge-conjugate processes are included unless otherwise stated.

Details about BESIII and BEPCII can be found in Refs. [21–26]. High-statistics Monte Carlo (MC) simulation samples for the annihilation of $e^+e^- \rightarrow$ inclusive are generated with the KKMC generator [27] incorporating initial-state radiation (ISR) effects and the beam-energy spread. The inclusive MC sample, comprising $\Lambda_c^+\bar{\Lambda}_c^-$ events and hadronic processes such as $D_{(s)}^{(*)}$ production, ISR return to the lower-mass ψ states, and the continuum processes $e^+e^- \rightarrow q\bar{q}$ ($q = u, d, s$), is generat-

ed to determine ST detection efficiency and estimate the potential background. The sample has been validated to describe the data well. All particle decays are modelled with EVTGEN [28, 29] using BFs either taken from the Particle Data Group (PDG) [11], or estimated with LUNDCHARM when available [30]. Final-state particles are propagated through a GEANT4 based detector simulation, which provides an accurate geometric description of the BESIII detector [31, 32]. The Born cross sections are taken into account when generating $\Lambda_c^+\bar{\Lambda}_c^-$ pairs in inclusive MC samples [33]. Furthermore, signal MC samples are generated to determine the DT detection efficiencies, where the $\bar{\Lambda}_c^-$ decays into any of the tag modes and the Λ_c^+ decays inclusively into the modes containing a Λ in final states. These samples incorporate amplitude models for the dominating multi-body processes [34] (e.g., $\Lambda_c^+ \rightarrow \Lambda\pi^+\pi^0$) and account for angular distributions in two-body decays [35] (e.g., $\Lambda_c^+ \rightarrow \Lambda\pi^+$). To further improve the agreement between signal MC samples and data, key kinematic distributions, including the recoil mass against the Λ and the Λ momentum, are reweighted using the Boosted Decision Tree (BDT) algorithm [36].

The selection of ST $\bar{\Lambda}_c^-$ candidates follows the procedure described in Ref. [37]. The ST $\bar{\Lambda}_c^-$ candidates are reconstructed, and the beam-constrained mass is defined as $M_{BC} \equiv \sqrt{E_{\text{beam}}^2/c^4 - |\vec{p}|^2/c^2}$ to extract the ST yields. After reconstructing a $\bar{\Lambda}_c^-$ through one of the eleven ST modes, a Λ candidate is selected from the remaining tracks via the $\Lambda \rightarrow p\pi^-$ process, referred to as the DT candidate. The Λ candidates on the signal side are selected using the same criteria as those used for the Λ candidates reconstructed on the tag side. To obtain the pure signal shape, a truth-matching procedure based on reconstructed and simulated information is applied to the signal MC samples in the ST and DT sides. The matching angle θ_{match} of the $p\pi^-$ from Λ in the ST and DT sides must satisfy $\theta_{\text{match}}(p) < 15^\circ$ and $\theta_{\text{match}}(\pi^-) < 25^\circ$, and $\theta_{\text{match}} < 10^\circ$ is required for other particles in the ST side. Otherwise, they are considered as “unmatched events”.

To obtain the BF, a two-dimensional (2D) simultaneous unbinned maximum likelihood fit is performed to the distribution of M_{BC} versus the invariant mass of $p\pi^-$ (M_Λ) at seven center-of-mass energy points, with all ST modes combined at each energy point. The signal is modeled by the MC-simulated shape convolved with a Gaussian function with floating parameters to describe the detector resolution. The unmatched background is described using the shape taken from the signal MC samples. The ratio of matched to unmatched event numbers is fixed based on a study of the signal MC samples.

The background shape from $e^+e^- \rightarrow \Lambda_c^+\bar{\Lambda}_c^-$ is extracted from $\Lambda_c^+\bar{\Lambda}_c^-$ inclusive MC samples, and the ratio between the signal and $\Lambda_c^+\bar{\Lambda}_c^-$ background yields is also fixed in the fitting procedure by studying the inclusive MC samples. The background from hadronic process-

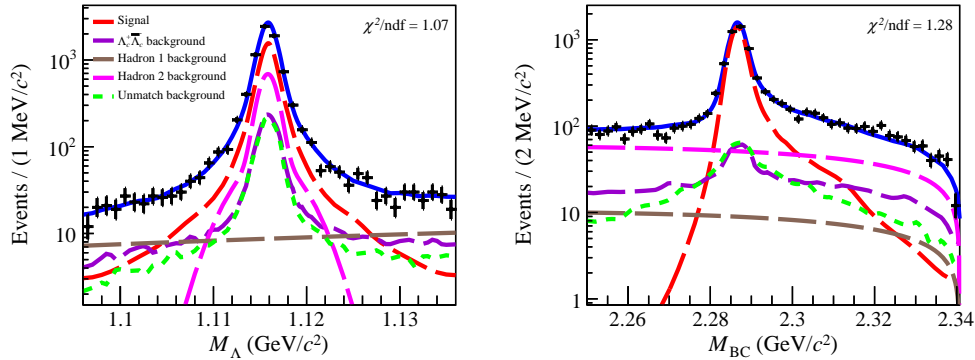


FIG. 1. Projections of the 2D simultaneous fit on the M_Λ versus M_{BC} distributions for the data taken at $\sqrt{s} = 4.682$ GeV, where the vertical axis is shown on a logarithmic scale. Points with error bars are data, the blue solid lines are the sum of the fitting functions, the red dashed lines are the signal, the purple dashed lines are the $\Lambda_c^+ \bar{\Lambda}_c^-$ background, the brown dashed lines are the “hadron 1” background, the magenta dashed lines are the “hadron 2” background and the green dashed lines are the unmatched background.

es can be classified into two categories: combinatorial background in both the M_Λ and M_{BC} distributions, and peaking background in the M_Λ distribution or in the M_{BC} distribution, referred to as “hadron 1” and “hadron 2”, respectively. The “hadron 1” component is represented by an ARGUS function in the M_{BC} distribution and a polynomial function in the M_Λ distribution, while the “hadron 2” component is represented by an ARGUS function in the M_{BC} distribution and a double Gaussian function in the M_Λ distribution. The parameters of these functions are obtained by fitting the distribution of M_Λ versus M_{BC} of the hadron MC samples at each energy point, keeping the endpoint of the ARGUS function fixed to E_{beam} . The yields of the “hadron 1” and “hadron 2” components are free in the fit.

Figure 1 shows the fit result of the M_Λ versus M_{BC} distribution for data taken at $\sqrt{s} = 4.682$ GeV. The fit results displayed with linear vertical axes for all energies are shown in the Supplemental Material. In the fit, the BF of $\Lambda_c^+ \rightarrow \Lambda X$ is a common parameter at all energy points. The signal yields at each energy point are given as $N_j^{\text{DT}} = \mathcal{B} \cdot \sum_i N_{ij}^{\text{ST}} \cdot (\epsilon_{ij}^{\text{DT}} / \epsilon_{ij}^{\text{ST}}) \cdot \mathcal{B}_{\text{int}}$, where \mathcal{B} is the BF of $\Lambda_c^+ \rightarrow \Lambda X$, i and j represent the ST modes and the data samples at different center-of-mass energies, respectively, and the factor \mathcal{B}_{int} is $(64.1 \pm 0.5)\%$, which is the BF of $\Lambda \rightarrow p\pi^-$ [11]. N_{ij}^{ST} , $\epsilon_{ij}^{\text{ST}}$, and $\epsilon_{ij}^{\text{DT}}$ are the ST yields, ST efficiencies, and DT efficiencies, respectively. The ST yields and ST efficiencies are cited from Ref. [37], since we use the same reconstructed criteria for ST $\bar{\Lambda}_c^-$ candidates. The $\epsilon_{ij}^{\text{DT}}$ are estimated from the signal MC samples. Furthermore, the control samples $J/\psi \rightarrow \bar{p}K^+\Lambda$ and $J/\psi \rightarrow \Lambda\bar{\Lambda}$ are used to study the Λ reconstruction efficiencies. The correction factors depending on the Λ momentum and $\cos\theta$ (where θ is the polar angle) are obtained by studying the difference of Λ reconstruction efficiencies between data and MC sim-

ulation of the control sample. We use them to correct the DT signal MC samples according to the Λ momentum and $\cos\theta$ distributions in the decay $\Lambda_c^+ \rightarrow \Lambda X$, and the difference between the corrected and uncorrected efficiencies is $(1.4 \pm 0.6)\%$. The corrected DT efficiencies for each energy point are summarized in the Supplemental Material. The BF of $\Lambda_c^+ \rightarrow \Lambda X$, averaged over charge conjugate modes, is determined to be $(38.07 \pm 0.38_{\text{stat}})\%$.

Most systematic uncertainties from the ST side are canceled in the determination of the BFs, while those originating from the signal side may introduce systematic biases. They arise mainly from Λ reconstruction, the intermediate BF of $\Lambda \rightarrow p\pi^-$, the 2D fit procedure, the ST $\bar{\Lambda}_c^-$ yield, the BDT reweighting, the MC statistics, and the unmatched background. The total systematic uncertainty is obtained by summing all sources in quadrature. Details are given in the Supplemental Material.

The longitudinal polarization of Λ hyperon is extracted from the angular distribution of $\Lambda_c^+ \rightarrow \Lambda X$ with $\Lambda \rightarrow p\pi^-$, which is shown in Fig. 2. As described in Ref. [17], the proton angular distribution in the parity-violating decay $\Lambda \rightarrow p\pi^-$ can be written in terms of a single helicity angle:

$$\frac{d\Gamma}{d\cos\theta_p} \propto 1 + \mathcal{P}_\Lambda \alpha_- \cos\theta_p, \quad (1)$$

where α_- is the decay asymmetry parameter of Λ in $\Lambda \rightarrow p\pi^-$. The helicity axis is chosen as the Λ flight direction in the Λ_c^+ rest frame, and θ_p is the angle, measured in the Λ rest frame, between the proton momentum and this axis. The parameter \mathcal{P}_Λ denotes the longitudinal polarization component of the Λ along the chosen helicity axis, averaged over all contributing $\Lambda_c^+ \rightarrow \Lambda X$ decay modes. For the charge conjugate decay $\bar{\Lambda}_c^- \rightarrow \bar{\Lambda} X$, the α_- and \mathcal{P}_Λ are replaced by α_+ and $\mathcal{P}_{\bar{\Lambda}}$, respectively.

A simultaneous unbinned maximum likelihood fit for the seven data samples is performed to determine the

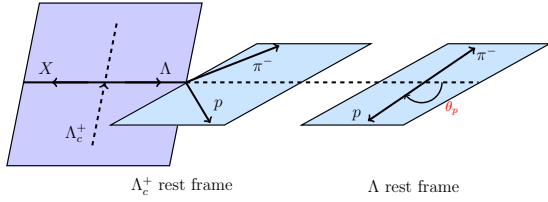


FIG. 2. Angular distribution of the inclusive decay $\Lambda_c^+ \rightarrow \Lambda X$ and its subsequent decay $\Lambda \rightarrow p\pi^-$.

common free parameter \mathcal{P}_Λ , following the procedure described in Ref. [38]. We construct the logarithmic likelihood function from the joint probability density function (PDF),

$$\ln \mathcal{L}_{\text{total}} = \sum \ln \mathcal{L}_{\text{energy}} = \sum \ln \left[\prod_{i=1}^{N_{\text{data}}} f_s(\theta_p^i) \right]. \quad (2)$$

Here, N_{data} is the number of events in the data and i is the event index. The PDF $f_s(\theta_p^i)$ is formulated as $f_s(\theta_p^i) = \frac{\epsilon(\theta_p^i) |M(\theta_p^i; \mathcal{P}_\Lambda)|^2}{\int \epsilon(\theta_p^i) |M(\theta_p^i; \mathcal{P}_\Lambda)|^2 d\theta_p^i}$, where $M(\theta_p^i; \mathcal{P}_\Lambda)$ is the angular distribution function described in Eq. (1) and $\epsilon(\theta_p^i)$ is the detection efficiency parameterized in terms of the kinematic variables θ_p^i . The integration of the normalization factor in the fitting procedure is calculated using a large BDT reweighted signal MC sample, with $\int \epsilon(\theta_p^i) |M(\theta_p^i; \mathcal{P}_\Lambda)|^2 d\theta_p^i \propto \frac{1}{N_{\text{gen}}} \sum_{k_{\text{MC}}}^{N_{\text{MC}}} |M(\theta_p^{k_{\text{MC}}}; \mathcal{P}_\Lambda)|^2$, where N_{gen} is the total number of the simulated signal MC events, N_{MC} is the number of the reweighted signal MC events surviving all selection criteria and k_{MC} is the event index. The contributions of the background component are subtracted based on the 2D data sideband when we calculate the joint likelihood, where the ratio between sideband and signal region events is calculated from the 2D simultaneous fit. A correction is applied to the $\cos \theta_p$ distribution of the data sideband events, accounting for the observed difference between the signal and the sideband regions in the background MC samples, which include contributions from $\Lambda_c^+ \Lambda_c^-$ pairs, hadronic processes, and unmatched components. As shown in Fig. 3, the box labeled S stands for the signal region, while boxes A, B, C, D and E represent the 2D sideband regions. In the M_{BC} distribution, only the lower sidebands are used, since the high side ISR tail contains signal events that would contaminate the background estimate.

The negative logarithmic likelihood with background subtraction over the seven data samples is minimized using the MINUIT package [39]. Here, $\alpha_- = 0.746 \pm 0.008$ and $\alpha_+ = -0.758 \pm 0.005$ are fixed to the PDG values [11]. Figure 4 shows the fitting results for the decays $\Lambda_c^+ \rightarrow \Lambda X$ and $\Lambda_c^- \rightarrow \bar{\Lambda} X$. Finally, we obtain $\mathcal{P}_\Lambda = -0.393 \pm 0.055_{\text{sta.}}$ and $\mathcal{P}_{\bar{\Lambda}} = 0.288 \pm 0.056_{\text{sta.}}$

Systematic uncertainties from imperfect simulation and the measurement method can affect the determina-

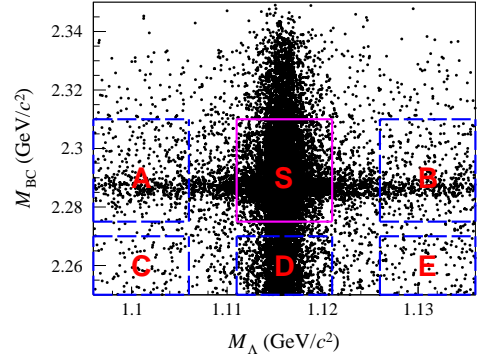


FIG. 3. Distribution of M_{BC} versus M_Λ in data taken at $\sqrt{s} = 4.682$ GeV. The Λ signal region is defined as (1.111, 1.121) GeV/c^2 , with sidebands taken as (1.096, 1.106) \cup (1.126, 1.136) GeV/c^2 , while the M_{BC} signal and sideband regions are chosen as (2.275, 2.31) GeV/c^2 and (2.25, 2.27) GeV/c^2 , respectively.

tion of Λ polarization. The main sources are the Λ reconstruction, the choice of the M_{BC} and M_Λ signal regions, the background subtraction, the unmatched background model, the input $\alpha_- (\alpha_+)$ parameters, and the MC model. All sources are added in quadrature to obtain the total systematic uncertainty and the details are provided in the Supplemental Material.

The direct CP asymmetry between $\Lambda_c^+ \rightarrow \Lambda X$ and $\bar{\Lambda}_c^- \rightarrow \bar{\Lambda} X$ can be written as $\mathcal{A}_{\text{CP}}^{\text{dir}} \equiv [\mathcal{B}(\Lambda_c^+ \rightarrow \Lambda X) - \mathcal{B}(\bar{\Lambda}_c^- \rightarrow \bar{\Lambda} X)] / [\mathcal{B}(\Lambda_c^+ \rightarrow \Lambda X) + \mathcal{B}(\bar{\Lambda}_c^- \rightarrow \bar{\Lambda} X)]$. Employing the same fitting procedure described earlier, we determine the BFs of the decays $\Lambda_c^+ \rightarrow \Lambda X$ and $\bar{\Lambda}_c^- \rightarrow \bar{\Lambda} X$ to be $(38.35 \pm 0.53_{\text{sta.}} \pm 0.69_{\text{sys.}})\%$ and $(37.19 \pm 0.53_{\text{sta.}} \pm 0.56_{\text{sys.}})\%$, respectively. The ST yields, ST efficiencies, and DT efficiencies of the charge conjugate decays are summarized in Supplemental Material. Using the separate BFs of the charge conjugate decays, the direct CP asymmetry is calculated to be $\mathcal{A}_{\text{CP}}^{\text{dir}} = (1.5 \pm 1.0_{\text{sta.}} \pm 1.0_{\text{sys.}})\%$. In the evaluation of the systematic uncertainty, the contribution from the intermediate BF of $\Lambda \rightarrow p\pi^-$ is treated as fully correlated between the charge conjugate modes. This result is consistent with the previous measurement [12], with a precision improved by nearly a factor of four. The CP asymmetry constructed from the Λ polarization and decay asymmetry parameters, $\mathcal{A}_{\text{CP}}^{\text{pol}} \equiv (\mathcal{P}_\Lambda \alpha_- - \mathcal{P}_{\bar{\Lambda}} \alpha_+) / (\mathcal{P}_\Lambda \alpha_- + \mathcal{P}_{\bar{\Lambda}} \alpha_+)$, provides access to baryon CPV in the inclusive decay $\Lambda_c^+ \rightarrow \Lambda X$, which is therefore polarization dependent. We obtain $\mathcal{A}_{\text{CP}}^{\text{pol}} = 0.15 \pm 0.12_{\text{sta.}} \pm 0.04_{\text{sys.}}$. This is the first time to search for polarization-dependent CPV in the Λ_c^+ inclusive decay.

In summary, using data corresponding to an integrated luminosity of 4.5 fb^{-1} , collected by BESIII at center-of-mass energies between 4.600 and 4.699 GeV, we determine the longitudinal polarization of Λ and $\bar{\Lambda}$ hyperons produced in $\Lambda_c^+ \rightarrow \Lambda X$ and $\bar{\Lambda}_c^- \rightarrow \bar{\Lambda} X$ for

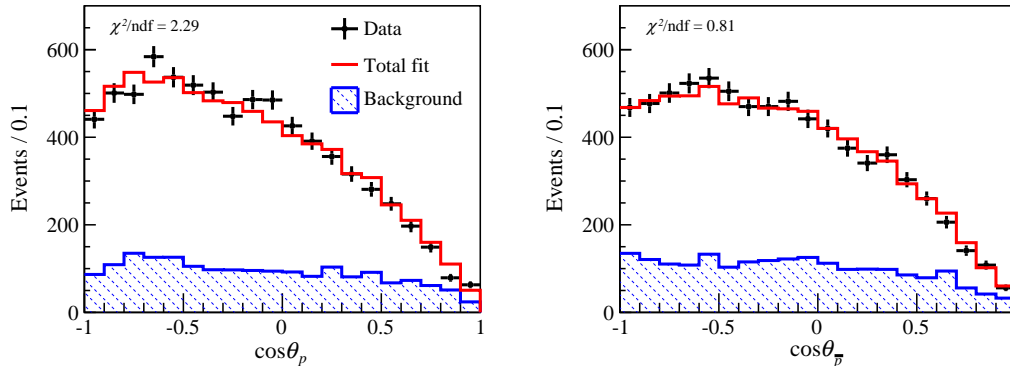


FIG. 4. The angular distributions for (left) $\Lambda_c^+ \rightarrow \Lambda X$ and (right) $\bar{\Lambda}_c^- \rightarrow \bar{\Lambda} X$, obtained by summing over the data samples of all the energy points. Points with error bars are data, the red lines are the fitting models, and the blue shaded areas are the background events of the 2D sideband region in data.

the first time to be $-0.393 \pm 0.055_{\text{sta.}} \pm 0.020_{\text{sys.}}$ and $0.288 \pm 0.056_{\text{sta.}} \pm 0.017_{\text{sys.}}$. These results provide detailed information that improves our understanding of the dynamics of charm baryon decay. Then, the absolute BF of the inclusive decay $\Lambda_c^+ \rightarrow \Lambda X$ is determined to be $\mathcal{B}(\Lambda_c^+ \rightarrow \Lambda X) = (38.07 \pm 0.38_{\text{sta.}} \pm 0.49_{\text{sys.}})\%$, with precision improved by a factor of four, over the previous BESIII measurement [12]. This more precise determination constrains the sum of known exclusive Λ_c^+ decay channels, thereby reducing the allowed phase space for yet-undiscovered modes and providing a target for future searches. By comparing with the measured exclusive processes containing Λ in the final states listed in the PDG, it is found that $(6.71 \pm 1.25)\%$ of the exclusive decays remain unmeasured. Moreover, we measure the direct CP asymmetry to be $\mathcal{A}_{\text{CP}}^{\text{dir}} = (1.5 \pm 1.0_{\text{sta.}} \pm 1.0_{\text{sys.}})\%$. We also perform the first search for the polarization-dependent CPV in this inclusive decay process, obtaining $\mathcal{A}_{\text{CP}}^{\text{pol}} = 0.15 \pm 0.12_{\text{sta.}} \pm 0.04_{\text{sys.}}$. By searching for the CPV in inclusive mode, we provide a complementary constraint on a net CPV in $\Lambda_c^+ \rightarrow \Lambda X$ decays that survives after integration over all contributing subchannels, which is relevant for understanding the mechanisms underlying the baryon asymmetry of the universe.

The BESIII Collaboration thanks the staff of BEPCII (<https://cstr.cn/31109.02.BEPC>) and the IHEP computing center for their strong support. This work is supported in part by National Key R&D Program of China under Contracts Nos. 2023YFA1609400, 2023YFA1606000, 2023YFA1606704; National Natural Science Foundation of China (NSFC) under Contracts Nos. 12105127, 12422504, 11635010, 11935015, 11935016, 11935018, 12025502, 12035009, 12035013, 12061131003, 12192260, 12192261, 12192262, 12192263, 12192264, 12192265, 12221005, 12225509, 12235017, 12342502, 12361141819; the Chinese Academy of Sciences (CAS) Large-Scale Scientific Facility Program; the Strategic Priority Research Program of Chinese Academy of Sciences un-

der Contract No. XDA0480600; CAS under Contract No. YSBR-101; 100 Talents Program of CAS; Fundamental Research Funds for the Central Universities, Lanzhou University under Contracts Nos. lzujbky-2025-ytB01, lzujbky-2023-stlt01; The Institute of Nuclear and Particle Physics (INPAC) and Shanghai Key Laboratory for Particle Physics and Cosmology; ERC under Contract No. 758462; German Research Foundation DFG under Contract No. FOR5327; Istituto Nazionale di Fisica Nucleare, Italy; Knut and Alice Wallenberg Foundation under Contracts Nos. 2021.0174, 2021.0299, 2023.0315; Ministry of Development of Turkey under Contract No. DPT2006K-120470; National Research Foundation of Korea under Contract No. NRF-2022R1A2C1092335; National Science and Technology fund of Mongolia; Polish National Science Centre under Contract No. 2024/53/B/ST2/00975; STFC (United Kingdom); Swedish Research Council under Contract No. 2019.04595; U. S. Department of Energy under Contract No. DE-FG02-05ER41374

-
- [1] A. D. Sakharov, *Pisma Zh. Eksp. Teor. Fiz.* **5**, 32 (1967).
 - [2] J. H. Christenson, J. W. Cronin, V. L. Fitch and R. Turlay, *Phys. Rev. Lett.* **13**, 138 (1964).
 - [3] B. Aubert *et al.* (BaBar Collaboration), *Phys. Rev. Lett.* **87**, 091801 (2001).
 - [4] K. Abe *et al.* (Belle Collaboration), *Phys. Rev. Lett.* **87**, 091802 (2001).
 - [5] R. Aaij *et al.* (LHCb Collaboration), *Phys. Rev. Lett.* **122**, 211803 (2019).
 - [6] R. Aaij *et al.* (LHCb Collaboration), *Nature* **643**, 1223 (2025).
 - [7] H. Y. Cheng and C. W. Chiang, *Phys. Rev. D* **85**, 034036 (2012).
 - [8] H. Y. Cheng, *Chin. J. Phys.* **78**, 324 (2022).
 - [9] P. R. Li, X. R. Lyu and Y. H. Zheng, *Chin. Phys.* **50**, 022002 (2026).

- [10] S. Capstick and W. Roberts, *Prog. Part. Nucl. Phys.* **45**, S241 (2000).
- [11] S. Navas *et al.* (Particle Data Group), *Phys. Rev. D* **110**, 030001 (2024) and 2025 update.
- [12] M. Ablikim *et al.* (BESIII Collaboration), *Phys. Rev. Lett.* **121**, 062003 (2018).
- [13] A. F. Falk and M. Neubert, *Phys. Rev. D* **47**, 2982 (1993).
- [14] H. J. Wang, P. R. Li, X. R. Lyu, J. Tandean and H. B. Li, *Sci. Bull.* **70**, 1183 (2025).
- [15] R. Aaij *et al.* (LHCb Collaboration), *Phys. Rev. Lett.* **133**, 261804 (2024).
- [16] L. K. Li *et al.* (Belle Collaboration), *Sci. Bull.* **68**, 583 (2023).
- [17] J. P. Wang and F. S. Yu, *Phys. Lett. B* **849**, 138460 (2024).
- [18] J. Adler *et al.* (MARKIII Collaboration), *Phys. Rev. Lett.* **62**, 1821 (1989).
- [19] M. Ablikim *et al.* (BESIII Collaboration), *Chin. Phys. C* **46**, 113002 (2022).
- [20] M. Ablikim *et al.* (BESIII Collaboration), *Chin. Phys. C* **46**, 113003 (2022).
- [21] M. Ablikim *et al.* (BESIII Collaboration), *Nucl. Instrum. Meth. A* **614**, 345 (2010).
- [22] C. Yu *et al.*, in *Proceedings of IPAC2016, Busan, Korea* (JACoW, Geneva, Switzerland, 2016), p. TUYA01.
- [23] M. Ablikim *et al.* (BESIII Collaboration), *Chin. Phys. C* **44**, 040001 (2020).
- [24] X. Li *et al.*, *Radiat. Detect. Technol. Methods* **1**, 13 (2017).
- [25] Y. X. Guo *et al.*, *Radiat. Detect. Technol. Methods* **1**, 15 (2017).
- [26] P. Cao *et al.*, *Nucl. Instrum. Meth. A* **953**, 163053 (2020).
- [27] S. Jadach, B. F. L. Ward, and Z. Was, *Phys. Rev. D* **63**, 113009 (2001).
- [28] D. J. Lange, *Nucl. Instrum. Meth. A* **462**, 152 (2001).
- [29] R. G. Ping, *Chin. Phys. C* **32**, 599 (2008).
- [30] J. C. Chen, G. S. Huang, X. R. Qi, D. H. Zhang, and Y. S. Zhu, *Phys. Rev. D* **62**, 034003 (2000); R. L. Yang, R. G. Ping and H. Chen, *Chin. Phys. Lett.* **31**, 061301 (2014).
- [31] S. Agostinelli *et al.* (GEANT4 Collaboration), *Nucl. Instrum. Meth. A* **506**, 250 (2003).
- [32] J. Allison *et al.*, *IEEE Trans. Nucl. Sci.* **53**, 270 (2006).
- [33] M. Ablikim *et al.* (BESIII Collaboration), *Phys. Rev. Lett.* **131**, 191901 (2023).
- [34] M. Ablikim *et al.* (BESIII Collaboration), *JHEP* **12**, 033 (2022).
- [35] M. Ablikim *et al.* (BESIII Collaboration), *arXiv:2508.11400*.
- [36] A. Rogozhnikov, *J. Phys. Conf. Ser.* **762**, 012036 (2016).
- [37] M. Ablikim *et al.* (BESIII Collaboration), *Chin. Phys. C* **47**, 023001 (2023).
- [38] M. Ablikim *et al.* (BESIII Collaboration), *Phys. Rev. Lett.* **132**, 031801 (2024).
- [39] F. James and M. Roos, *Comput. Phys. Commun.* **10**, 343 (1975).

Supplemental Material for “Precision Studies and Searches for CP Asymmetries in the Inclusive Decay $\Lambda_c^+ \rightarrow \Lambda X$ ”

M. Ablikim¹, M. N. Achasov^{4,c}, P. Adlarson⁸¹, X. C. Ai⁸⁷, C. S. Akondi^{31A,31B}, R. Aliberti³⁹, A. Amoroso^{80A,80C}, Q. An^{77,64,†}, Y. H. An⁸⁷, Y. Bai⁶², O. Bakina⁴⁰, Y. Ban^{50,h}, H.-R. Bao⁷⁰, X. L. Bao⁴⁹, V. Batzskaya^{1,48}, K. Begzsuren³⁵, N. Berger³⁹, M. Berlowski⁴⁸, M. B. Bertani^{30A}, D. Bettoni^{31A}, F. Bianchi^{80A,80C}, E. Bianco^{80A,80C}, A. Bortone^{80A,80C}, I. Boyko⁴⁰, R. A. Briere⁵, A. Brueggemann⁷⁴, H. Cai⁸², M. H. Cai^{42,k,l}, X. Cai^{1,64}, A. Calcaterra^{30A}, G. F. Cao^{1,70}, N. Cao^{1,70}, S. A. Cetin^{68A}, X. Y. Chai^{50,h}, J. F. Chang^{1,64}, T. T. Chang⁴⁷, M. L. Chen^{1,64,70}, G. R. Che⁴⁷, Y. Z. Che^{1,64,70}, C. H. Chen¹⁰, Chao Chen¹, G. Chen¹, H. S. Chen^{1,70}, H. Y. Chen²¹, M. L. Chen^{1,64,70}, S. J. Chen⁴⁶, S. M. Chen⁶⁷, T. Chen^{1,70}, W. Chen⁴⁹, X. R. Chen^{34,70}, X. T. Chen^{1,70}, X. Y. Chen^{12,g}, Y. B. Chen^{1,64}, Y. Q. Chen¹⁶, Z. K. Chen⁶⁵, J. Cheng⁴⁹, L. N. Cheng⁴⁷, S. K. Choi¹¹, X. Chu^{12,g}, G. Cibinetto^{31A}, F. Cossio^{80C}, J. Cottee-Meldrum⁶⁹, H. L. Dai^{1,64}, J. P. Dai⁸⁵, X. C. Dai⁶⁷, A. Dbeyssi¹⁹, R. E. de Boer³, D. Dedovich⁴⁰, C. Q. Deng⁷⁸, Z. Y. Deng¹, A. Denig³⁹, I. Denisenko⁴⁰, M. Destefanis^{80A,80C}, F. De Mori^{80A,80C}, X. X. Ding^{50,h}, Y. Ding⁴⁴, Y. X. Ding³², J. Dong^{1,64}, L. Y. Dong^{1,70}, M. Y. Dong^{1,64,70}, X. Dong⁸², M. C. Du¹, S. X. Du⁸⁷, S. X. Du^{12,g}, X. L. Du^{12,g}, Y. Q. Du⁸², Y. Y. Duan⁶⁰, Z. H. Duan⁴⁶, P. Egorov^{40,b}, G. F. Fan⁴⁶, J. J. Fan²⁰, Y. H. Fan⁴⁹, J. Fang^{1,64}, J. Fang⁶⁵, S. S. Fang^{1,70}, W. X. Fang¹, Y. Q. Fang^{1,64,†}, L. Fava^{80B,80C}, F. Feldbauer³, G. Felici^{30A}, C. Q. Feng^{77,64}, J. H. Feng¹⁶, L. Feng^{42,k,l}, Q. X. Feng^{42,k,l}, Y. T. Feng^{77,64}, M. Fritsch³, C. D. Fu¹, J. L. Fu⁷⁰, Y. W. Fu^{1,70}, H. Gao⁷⁰, Y. Gao^{77,64}, Y. N. Gao^{50,h}, Y. N. Gao²⁰, Y. Y. Gao³², Z. Gao⁴⁷, S. Garbolino^{80C}, I. Garzia^{31A,31B}, L. Ge⁶², P. T. Ge²⁰, Z. W. Ge⁴⁶, C. Geng⁶⁵, E. M. Gersabeck⁷³, A. Gilman⁷⁵, K. Goetzen¹³, J. Gollub³, J. B. Gong^{1,70}, J. D. Gong³⁸, L. Gong⁴⁴, W. X. Gong^{1,64}, W. Gradl³⁹, S. Gramigna^{31A,31B}, M. Greco^{80A,80C}, M. D. Gu⁵⁵, M. H. Gu^{1,64}, C. Y. Guan^{1,70}, A. Q. Guo³⁴, J. N. Guo^{12,g}, L. B. Guo⁴⁵, M. J. Guo⁵⁴, R. P. Guo⁵³, X. Guo⁵⁴, Y. P. Guo^{12,g}, Z. Guo^{77,64}, A. Guskov^{40,b}, J. Gutierrez²⁹, J. Y. Han^{77,64}, T. T. Han¹, X. Han^{77,64}, F. H. Hansch³, K. D. Hao^{77,64}, X. Q. Hao²⁰, F. A. Harris⁷¹, C. Z. He^{50,h}, K. K. He⁶⁰, K. L. He^{1,70}, F. H. Heinsius³, C. H. Heinz³⁹, Y. K. Heng^{1,64,70}, C. Herold⁶⁶, P. C. Hong³⁸, G. Y. Hou^{1,70}, X. T. Hou^{1,70}, Y. R. Hou⁷⁰, Z. L. Hou¹, H. M. Hu^{1,70}, J. F. Hu^{61,j}, Q. P. Hu^{77,64}, S. L. Hu^{12,g}, T. Hu^{1,64,70}, Y. Hu¹, Y. X. Hu⁸², Z. M. Hu⁶⁵, G. S. Huang^{77,64}, K. X. Huang⁶⁵, L. Q. Huang^{34,70}, P. Huang⁴⁶, X. T. Huang⁵⁴, Y. P. Huang¹, Y. S. Huang⁶⁵, T. Hussain⁷⁹, N. Hüsken³⁹, N. in der Wiesche⁷⁴, J. Jackson²⁹, Q. Ji¹, Q. P. Ji²⁰, W. Ji^{1,70}, X. B. Ji^{1,70}, X. L. Ji^{1,64}, L. K. Jia⁷⁰, X. Q. Jia⁵⁴, Z. K. Jia^{77,64}, D. Jiang^{1,70}, H. B. Jiang⁸², P. C. Jiang^{50,h}, S. J. Jiang¹⁰, X. S. Jiang^{1,64,70}, Y. Jiang⁷⁰, J. B. Jiao⁵⁴, J. K. Jiao³⁸, Z. Jiao²⁵, L. C. L. Jin¹, S. Jin⁴⁶, Y. Jin⁷², M. Q. Jing^{1,70}, X. M. Jing⁷⁰, T. Johansson⁸¹, S. Kabana³⁶, X. L. Kang¹⁰, X. S. Kang⁴⁴, B. C. Ke⁸⁷, V. Khachatryan²⁹, A. Khoukaz⁷⁴, O. B. Kolcu^{68A}, B. Kopf³, L. Kröger⁷⁴, L. Krümmel³, Y. Y. Kuang⁷⁸, M. Kuessner³, X. Kui^{1,70}, N. Kumar²⁸, A. Kupsc^{48,81}, W. Kühn⁴¹, Q. Lan⁷⁸, W. N. Lan²⁰, T. T. Lei^{77,64}, M. Lellmann³⁹, T. Lenz³⁹, C. Li⁵¹, C. Li⁴⁷, C. H. Li⁴⁵, C. K. Li²¹, C. K. Li⁴⁷, D. M. Li⁸⁷, F. Li^{1,64}, G. Li¹, H. B. Li^{1,70}, H. J. Li²⁰, H. L. Li⁸⁷, H. N. Li^{61,j}, H. P. Li⁴⁷, Hui Li⁴⁷, J. S. Li⁶⁵, J. W. Li⁵⁴, K. Li¹, K. L. Li^{42,k,l}, L. J. Li^{1,70}, Lei Li⁵², M. H. Li⁴⁷, M. R. Li^{1,70}, P. L. Li⁷⁰, P. R. Li^{42,k,l}, Q. M. Li^{1,70}, Q. X. Li⁵⁴, R. Li^{18,34}, S. Li⁸⁷, S. X. Li¹², S. Y. Li⁸⁷, Shanshan Li^{27,i}, T. Li⁵⁴, T. Y. Li⁴⁷, W. D. Li^{1,70}, W. G. Li^{1,†}, X. Li^{1,70}, X. H. Li^{77,64}, X. K. Li^{50,h}, X. L. Li⁵⁴, X. Y. Li^{1,9}, X. Z. Li⁶⁵, Y. Li²⁰, Y. G. Li⁷⁰, Y. P. Li³⁸, Z. H. Li⁴², Z. J. Li⁶⁵, Z. L. Li⁸⁷, Z. X. Li⁴⁷, Z. Y. Li⁸⁵, C. Liang⁴⁶, H. Liang^{77,64}, Y. F. Liang⁵⁹, Y. T. Liang^{34,70}, G. R. Liao¹⁴, L. B. Liao⁶⁵, M. H. Liao⁶⁵, Y. P. Liao^{1,70}, J. Libby²⁸, A. Limphirat⁶⁶, C. C. Lin⁶⁰, D. X. Lin^{34,70}, T. Lin¹, B. J. Liu¹, B. X. Liu⁸², C. Liu³⁸, C. X. Liu¹, F. Liu¹, F. H. Liu⁵⁸, Feng Liu⁶, G. M. Liu^{61,j}, H. Liu^{42,k,l}, H. B. Liu¹⁵, H. M. Liu^{1,70}, Huihui Liu²², J. B. Liu^{77,64}, J. J. Liu²¹, K. Liu^{42,k,l}, K. Liu⁷⁸, K. Y. Liu⁴⁴, Ke Liu²³, L. Liu⁴², L. C. Liu⁴⁷, Lu Liu⁴⁷, M. H. Liu³⁸, P. L. Liu⁵⁴, Q. Liu⁷⁰, S. B. Liu^{77,64}, T. Liu¹, W. M. Liu^{77,64}, W. T. Liu⁴³, X. Liu^{42,k,l}, X. K. Liu^{42,k,l}, X. L. Liu^{12,g}, X. P. Liu^{12,g}, X. Y. Liu⁸², Y. Liu^{42,k,l}, Y. Liu⁸⁷, Y. B. Liu⁴⁷, Z. A. Liu^{1,64,70}, Z. D. Liu⁸³, Z. L. Liu⁷⁸, Z. Q. Liu⁵⁴, Z. Y. Liu⁴², X. C. Lou^{1,64,70}, H. J. Lu²⁵, J. G. Lu^{1,64}, X. L. Lu¹⁶, Y. Lu⁷, Y. H. Lu^{1,70}, Y. P. Lu^{1,64}, Z. H. Lu^{1,70}, C. L. Luo⁴⁵, J. R. Luo⁶⁵, J. S. Luo^{1,70}, M. X. Luo⁸⁶, T. Luo^{12,g}, X. L. Luo^{1,64}, Z. Y. Lv²³, X. R. Lyu^{70,o}, Y. F. Lyu⁴⁷, Y. H. Lyu⁸⁷, F. C. Ma⁴⁴, H. L. Ma¹, Heng Ma^{27,i}, J. L. Ma^{1,70}, L. L. Ma⁵⁴, L. R. Ma⁷², Q. M. Ma¹, R. Q. Ma^{1,70}, R. Y. Ma²⁰, T. Ma^{77,64}, X. T. Ma^{1,70}, X. Y. Ma^{1,64}, Y. M. Ma³⁴, F. E. Maas¹⁹, I. MacKay⁷⁵, M. Maggiora^{80A,80C}, S. Malde⁷⁵, Q. A. Malik⁷⁹, H. X. Mao^{42,k,l}, Y. J. Mao^{50,h}, Z. P. Mao¹, S. Marcello^{80A,80C}, A. Marshall⁶⁹, F. M. Melendi^{31A,31B}, Y. H. Meng⁷⁰, Z. X. Meng⁷², G. Mezzadri^{31A}, H. Miao^{1,70}, T. J. Min⁴⁶, R. E. Mitchell²⁹, X. H. Mo^{1,64,70}, B. Moses²⁹, N. Yu. Muchnoi^{4,c}, J. Muskalla³⁹, Y. Nefedov⁴⁰, F. Nerling^{19,e}, H. Neuwirth⁷⁴, Z. Ning^{1,64}, S. Nisar^{33,a}, Q. L. Niu^{42,k,l}, W. D. Niu^{12,g}, Y. Niu⁵⁴, C. Normand⁶⁹, S. L. Olsen^{11,70}, Q. Ouyang^{1,64,70}, S. Pacetti^{30B,30C}, X. Pan⁶⁰, Y. Pan⁶², A. Pathak¹¹, Y. P. Pei^{77,64}, M. Pelizaeus³, G. L. Peng^{77,64}, H. P. Peng^{77,64}, X. J. Peng^{42,k,l}, Y. Y. Peng^{42,k,l}, K. Peters^{13,e}, K. Petridis⁶⁹, J. L. Ping⁴⁵, R. G. Ping^{1,70}, S. Plura³⁹, V. Prasad³⁸, F. Z. Qi¹, H. R. Qi⁶⁷, M. Qi⁴⁶, S. Qian^{1,64}, W. B. Qian⁷⁰, C. F. Qiao⁷⁰, J. H. Qiao²⁰, J. J. Qin⁷⁸, J. L. Qin⁶⁰, L. Q. Qin¹⁴, L. Y. Qin^{77,64}, P. B. Qin⁷⁸, X. P. Qin⁴³, X. S. Qin⁵⁴, Z. H. Qin^{1,64}, J. F. Qiu¹, Z. H. Qu⁷⁸, J. Rademacker⁶⁹, C. F. Redmer³⁹, A. Rivetti^{80C}, M. Rolo^{80C}, G. Rong^{1,70}, S. S. Rong^{1,70}, F. Rosini^{30B,30C}, Ch. Rosner¹⁹, M. Q. Ruan^{1,64}, N. Salone^{48,p}, A. Sarantsev^{40,d}, Y. Schelhaas³⁹, K. Schoenning⁸¹, M. Scodeggio^{31A}, W. Shan²⁶, X. Y. Shan^{77,64}, Z. J. Shang^{42,k,l}, J. F. Shangguan¹⁷, L. G. Shao^{1,70}, M. Shao^{77,64}, C. P. Shen^{12,g}, H. F. Shen^{1,9}, W. H. Shen⁷⁰,

X. Y. Shen^{1,70} , B. A. Shi⁷⁰ , H. Shi^{77,64} , J. L. Shi^{8,q} , J. Y. Shi¹ , M. H. Shi⁸⁷ , S. Y. Shi⁷⁸ , X. Shi^{1,64} ,
H. L. Song^{77,64} , J. J. Song²⁰ , M. H. Song⁴² , T. Z. Song⁶⁵ , W. M. Song³⁸ , Y. X. Song^{50,h,m} , Ziron Song^{27,i} ,
S. Sosio^{80A,80C} , S. Spataro^{80A,80C} , S. Stansilau⁷⁵ , F. Stieler³⁹ , M. Stolte³ , S. S. Su⁴⁴ , G. B. Sun⁸² ,
G. X. Sun¹ , H. Sun⁷⁰ , H. K. Sun¹ , J. F. Sun²⁰ , K. Sun⁶⁷ , L. Sun⁸² , R. Sun⁷⁷ , S. S. Sun^{1,70} , T. Sun^{56,f} ,
W. Y. Sun⁵⁵ , Y. C. Sun⁸² , Y. H. Sun³² , Y. J. Sun^{77,64} , Y. Z. Sun¹ , Z. Q. Sun^{1,70} , Z. T. Sun⁵⁴ , C. J. Tang⁵⁹,
G. Y. Tang¹ , J. Tang⁶⁵ , J. J. Tang^{77,64} , L. F. Tang⁴³ , Y. A. Tang⁸² , L. Y. Tao⁷⁸ , M. Tat⁷⁵ ,
J. X. Teng^{77,64} , J. Y. Tian^{77,64} , W. H. Tian⁶⁵ , Y. Tian³⁴ , Z. F. Tian⁸² , I. Uman^{68B} , E. van der Smagt³ ,
B. Wang¹ , B. Wang⁶⁵ , Bo Wang^{77,64} , C. Wang^{42,k,l} , C. Wang²⁰ , Cong Wang²³ , D. Y. Wang^{50,h} ,
H. J. Wang^{42,k,l} , H. R. Wang⁸⁴ , J. Wang¹⁰ , J. J. Wang⁸² , J. P. Wang³⁷ , K. Wang^{1,64} , L. L. Wang¹ ,
L. W. Wang³⁸ , M. Wang⁵⁴ , M. Wang^{77,64} , N. Y. Wang⁷⁰ , S. Wang^{42,k,l} , Shun Wang⁶³ , T. Wang^{12,g} ,
T. J. Wang⁴⁷ , W. Wang⁶⁵ , W. P. Wang³⁹ , X. F. Wang^{42,k,l} , X. L. Wang^{12,g} , X. N. Wang^{1,70} , Xin Wang^{27,i} ,
Y. Wang¹ , Y. D. Wang⁴⁹ , Y. F. Wang^{1,9,70} , Y. H. Wang^{42,k,l} , Y. J. Wang^{77,64} , Y. L. Wang²⁰ , Y. N. Wang⁴⁹ ,
Y. N. Wang⁸² , Yaqian Wang¹⁸ , Yi Wang⁶⁷ , Yuan Wang^{18,34} , Z. Wang^{1,64} , Z. Wang⁴⁷ , Z. L. Wang² ,
Z. Q. Wang^{12,g} , Z. Y. Wang^{1,70} , Ziyi Wang⁷⁰ , D. Wei⁴⁷ , D. H. Wei¹⁴ , H. R. Wei⁴⁷ , F. Weidner⁷⁴ ,
S. P. Wen¹ , U. Wiedner³ , G. Wilkinson⁷⁵ , M. Wolke⁸¹ , J. F. Wu^{1,9} , L. H. Wu¹ , L. J. Wu²⁰ , Lianjie Wu²⁰ ,
S. G. Wu^{1,70} , S. M. Wu⁷⁰ , X. W. Wu⁷⁸ , Z. Wu^{1,64} , H. L. Xia^{77,64} , L. Xia^{77,64} , B. H. Xiang^{1,70} ,
D. Xiao^{42,k,l} , G. Y. Xiao⁴⁶ , H. Xiao⁷⁸ , Y. L. Xiao^{12,g} , Z. J. Xiao⁴⁵ , C. Xie⁴⁶ , K. J. Xie^{1,70} , Y. Xie⁵⁴ ,
Y. G. Xie^{1,64} , Y. H. Xie⁶ , Z. P. Xie^{77,64} , T. Y. Xing^{1,70} , D. B. Xiong¹ , C. J. Xu⁶⁵ , G. F. Xu¹ , H. Y. Xu² ,
M. Xu^{77,64} , Q. J. Xu¹⁷ , Q. N. Xu³² , T. D. Xu⁷⁸ , X. P. Xu⁶⁰ , Y. Xu^{12,g} , Y. C. Xu⁸⁴ , Z. S. Xu⁷⁰ ,
F. Yan²⁴ , L. Yan^{12,g} , W. B. Yan^{77,64} , W. C. Yan⁸⁷ , W. H. Yan⁶ , W. P. Yan²⁰ , X. Q. Yan^{12,g} ,
Y. Y. Yan⁶⁶ , H. J. Yang^{56,f} , H. L. Yang³⁸ , H. X. Yang¹ , J. H. Yang⁴⁶ , R. J. Yang²⁰ , Y. Yang^{12,g} ,
Y. H. Yang⁴⁶ , Y. H. Yang⁴⁷ , Y. M. Yang⁸⁷ , Y. Q. Yang¹⁰ , Y. Z. Yang²⁰ , Z. Y. Yang⁷⁸ , Z. P. Yao⁵⁴ ,
M. Ye^{1,64} , M. H. Ye^{9,i} , Z. J. Ye^{61,j} , Junhao Yin⁴⁷ , Z. Y. You⁶⁵ , B. X. Yu^{1,64,70} , C. X. Yu⁴⁷ , G. Yu¹³ ,
J. S. Yu^{27,i} , L. W. Yu^{12,g} , T. Yu⁷⁸ , X. D. Yu^{50,h} , Y. C. Yu⁸⁷ , Y. C. Yu⁴² , C. Z. Yuan^{1,70} , H. Yuan^{1,70} ,
J. Yuan³⁸ , J. Yuan⁴⁹ , L. Yuan² , M. K. Yuan^{12,g} , S. H. Yuan⁷⁸ , Y. Yuan^{1,70} , C. X. Yue⁴³ , Ying Yue²⁰ ,
A. A. Zafar⁷⁹ , F. R. Zeng⁵⁴ , S. H. Zeng⁶⁹ , X. Zeng^{12,g} , Yujie Zeng⁶⁵ , Y. J. Zeng^{1,70} , Y. C. Zhai⁵⁴ ,
Y. H. Zhan⁶⁵ , Shunan Zhang⁷⁵ , B. L. Zhang^{1,70} , B. X. Zhang^{1,†} , D. H. Zhang⁴⁷ , G. Y. Zhang²⁰ ,
G. Y. Zhang^{1,70} , H. Zhang^{77,64} , H. Zhang⁸⁷ , H. C. Zhang^{1,64,70} , H. H. Zhang⁶⁵ , H. Q. Zhang^{1,64,70} ,
H. R. Zhang^{77,64} , H. Y. Zhang^{1,64} , J. Zhang⁶⁵ , J. Zhang⁵² , J. J. Zhang⁵⁷ , J. L. Zhang²¹ , J. Q. Zhang⁴⁵ ,
J. S. Zhang^{12,g} , J. W. Zhang^{1,64,70} , J. X. Zhang^{42,k,l} , J. Y. Zhang¹ , J. Y. Zhang^{12,g} , J. Z. Zhang^{1,70} ,
Jianyu Zhang⁷⁰ , L. M. Zhang⁶⁷ , Lei Zhang⁴⁶ , N. Zhang³⁸ , P. Zhang^{1,9} , Q. Zhang²⁰ , Q. Y. Zhang³⁸ ,
Q. Z. Zhang⁷⁰ , R. Y. Zhang^{42,k,l} , S. H. Zhang^{1,70} , Shulei Zhang^{27,i} , X. M. Zhang¹ , X. Y. Zhang⁵⁴ ,
Y. Zhang¹ , Y. Zhang⁷⁸ , Y. T. Zhang⁸⁷ , Y. H. Zhang^{1,64} , Y. P. Zhang^{77,64} , Z. D. Zhang¹ , Z. H. Zhang¹ ,
Z. L. Zhang³⁸ , Z. L. Zhang⁶⁰ , Z. X. Zhang²⁰ , Z. Y. Zhang⁸² , Z. Y. Zhang⁴⁷ , Z. Y. Zhang⁴⁹ , Zh. Zh. Zhang²⁰ ,
G. Zhao¹ , J.-P. Zhao⁷⁰ , J. Y. Zhao^{1,70} , J. Z. Zhao^{1,64} , L. Zhao¹ , L. Zhao^{77,64} , M. G. Zhao⁴⁷ ,
R. P. Zhao⁷⁰ , S. J. Zhao⁸⁷ , Y. B. Zhao^{1,64} , Y. L. Zhao⁶⁰ , Y. P. Zhao⁴⁹ , Y. X. Zhao^{34,70} , Z. G. Zhao^{77,64} ,
A. Zhemchugov^{40,b} , B. Zheng⁷⁸ , B. M. Zheng³⁸ , J. P. Zheng^{1,64} , W. J. Zheng^{1,70} , W. Q. Zheng¹⁰ ,
X. R. Zheng²⁰ , Y. H. Zheng^{70,o} , B. Zhong⁴⁵ , C. Zhong²⁰ , H. Zhou^{39,54,n} , J. Q. Zhou³⁸ , S. Zhou⁶ ,
X. Zhou⁸² , X. K. Zhou⁶ , X. R. Zhou^{77,64} , X. Y. Zhou⁴³ , Y. X. Zhou⁸⁴ , Y. Z. Zhou^{12,g} , A. N. Zhu⁷⁰ ,
J. Zhu⁴⁷ , K. Zhu¹ , K. J. Zhu^{1,64,70} , K. S. Zhu^{12,g} , L. X. Zhu⁷⁰ , Lin Zhu²⁰ , S. H. Zhu⁷⁶ , T. J. Zhu^{12,g} ,
W. D. Zhu^{12,g} , W. J. Zhu¹ , W. Z. Zhu²⁰ , Y. C. Zhu^{77,6}

- ²¹ Henan University, Kaifeng 475004, People's Republic of China
- ²² Henan University of Science and Technology, Luoyang 471003, People's Republic of China
- ²³ Henan University of Technology, Zhengzhou 450001, People's Republic of China
- ²⁴ Hengyang Normal University, Hengyang 421001, People's Republic of China
- ²⁵ Huangshan College, Huangshan 245000, People's Republic of China
- ²⁶ Hunan Normal University, Changsha 410081, People's Republic of China
- ²⁷ Hunan University, Changsha 410082, People's Republic of China
- ²⁸ Indian Institute of Technology Madras, Chennai 600036, India
- ²⁹ Indiana University, Bloomington, Indiana 47405, USA
- ³⁰ INFN Laboratori Nazionali di Frascati, (A)INFN Laboratori Nazionali di Frascati, I-00044, Frascati, Italy; (B)INFN Sezione di Perugia, I-06100, Perugia, Italy; (C)University of Perugia, I-06100, Perugia, Italy
- ³¹ INFN Sezione di Ferrara, (A)INFN Sezione di Ferrara, I-44122, Ferrara, Italy; (B)University of Ferrara, I-44122, Ferrara, Italy
- ³² Inner Mongolia University, Hohhot 010021, People's Republic of China
- ³³ Institute of Business Administration, Karachi,
- ³⁴ Institute of Modern Physics, Lanzhou 730000, People's Republic of China
- ³⁵ Institute of Physics and Technology, Mongolian Academy of Sciences, Peace Avenue 54B, Ulaanbaatar 13330, Mongolia
- ³⁶ Instituto de Alta Investigación, Universidad de Tarapacá, Casilla 7D, Arica 1000000, Chile
- ³⁷ Jiangsu Ocean University, Lianyungang 222000, People's Republic of China
- ³⁸ Jilin University, Changchun 130012, People's Republic of China
- ³⁹ Johannes Gutenberg University of Mainz, Johann-Joachim-Becher-Weg 45, D-55099 Mainz, Germany
- ⁴⁰ Joint Institute for Nuclear Research, 141980 Dubna, Moscow region, Russia
- ⁴¹ Justus-Liebig-Universität Giessen, II. Physikalisches Institut, Heinrich-Buff-Ring 16, D-35392 Giessen, Germany
- ⁴² Lanzhou University, Lanzhou 730000, People's Republic of China
- ⁴³ Liaoning Normal University, Dalian 116029, People's Republic of China
- ⁴⁴ Liaoning University, Shenyang 110036, People's Republic of China
- ⁴⁵ Nanjing Normal University, Nanjing 210023, People's Republic of China
- ⁴⁶ Nanjing University, Nanjing 210093, People's Republic of China
- ⁴⁷ Nankai University, Tianjin 300071, People's Republic of China
- ⁴⁸ National Centre for Nuclear Research, Warsaw 02-093, Poland
- ⁴⁹ North China Electric Power University, Beijing 102206, People's Republic of China
- ⁵⁰ Peking University, Beijing 100871, People's Republic of China
- ⁵¹ Qufu Normal University, Qufu 273165, People's Republic of China
- ⁵² Renmin University of China, Beijing 100872, People's Republic of China
- ⁵³ Shandong Normal University, Jinan 250014, People's Republic of China
- ⁵⁴ Shandong University, Jinan 250100, People's Republic of China
- ⁵⁵ Shandong University of Technology, Zibo 255000, People's Republic of China
- ⁵⁶ Shanghai Jiao Tong University, Shanghai 200240, People's Republic of China
- ⁵⁷ Shanxi Normal University, Linfen 041004, People's Republic of China
- ⁵⁸ Shanxi University, Taiyuan 030006, People's Republic of China
- ⁵⁹ Sichuan University, Chengdu 610064, People's Republic of China
- ⁶⁰ Soochow University, Suzhou 215006, People's Republic of China
- ⁶¹ South China Normal University, Guangzhou 510006, People's Republic of China
- ⁶² Southeast University, Nanjing 211100, People's Republic of China
- ⁶³ Southwest University of Science and Technology, Mianyang 621010, People's Republic of China
- ⁶⁴ State Key Laboratory of Particle Detection and Electronics, Beijing 100049, Hefei 230026, People's Republic of China
- ⁶⁵ Sun Yat-Sen University, Guangzhou 510275, People's Republic of China
- ⁶⁶ Suranaree University of Technology, University Avenue 111, Nakhon Ratchasima 30000, Thailand
- ⁶⁷ Tsinghua University, Beijing 100084, People's Republic of China
- ⁶⁸ Turkish Accelerator Center Particle Factory Group, (A)Istinye University, 34010, Istanbul, Turkey; (B)Near East University, Nicosia, North Cyprus, 99138, Mersin 10, Turkey
- ⁶⁹ University of Bristol, H H Wills Physics Laboratory, Tyndall Avenue, Bristol, BS8 1TL, UK
- ⁷⁰ University of Chinese Academy of Sciences, Beijing 100049, People's Republic of China
- ⁷¹ University of Hawaii, Honolulu, Hawaii 96822, USA
- ⁷² University of Jinan, Jinan 250022, People's Republic of China
- ⁷³ University of Manchester, Oxford Road, Manchester, M13 9PL, United Kingdom
- ⁷⁴ University of Muenster, Wilhelm-Klemm-Strasse 9, 48149 Muenster, Germany
- ⁷⁵ University of Oxford, Keble Road, Oxford OX13RH, United Kingdom
- ⁷⁶ University of Science and Technology Liaoning, Anshan 114051, People's Republic of China
- ⁷⁷ University of Science and Technology of China, Hefei 230026, People's Republic of China
- ⁷⁸ University of South China, Hengyang 421001, People's Republic of China
- ⁷⁹ University of the Punjab, Lahore-54590, Pakistan
- ⁸⁰ University of Turin and INFN, (A)University of Turin, I-10125, Turin, Italy; (B)University of Eastern Piedmont, I-15121, Alessandria, Italy; (C)INFN, I-10125, Turin, Italy

⁸¹ Uppsala University, Box 516, SE-75120 Uppsala, Sweden

⁸² Wuhan University, Wuhan 430072, People's Republic of China

⁸³ Xi'an Jiaotong University, No.28 Xianning West Road, Xi'an, Shaanxi 710049, P.R. China

⁸⁴ Yantai University, Yantai 264005, People's Republic of China

⁸⁵ Yunnan University, Kunming 650500, People's Republic of China

⁸⁶ Zhejiang University, Hangzhou 310027, People's Republic of China

⁸⁷ Zhengzhou University, Zhengzhou 450001, People's Republic of China

† Deceased

^a Also at Bogazici University, 34342 Istanbul, Turkey

^b Also at the Moscow Institute of Physics and Technology, Moscow 141700, Russia

^c Also at the Novosibirsk State University, Novosibirsk, 630090, Russia

^d Also at the NRC "Kurchatov Institute", PNPI, 188300, Gatchina, Russia

^e Also at Goethe University Frankfurt, 60323 Frankfurt am Main, Germany

^f Also at Key Laboratory for Particle Physics, Astrophysics and Cosmology, Ministry of Education; Shanghai Key Laboratory for Particle Physics and Cosmology; Institute of Nuclear and Particle Physics, Shanghai 200240, People's Republic of China

^g Also at Key Laboratory of Nuclear Physics and Ion-beam Application (MOE) and Institute of Modern Physics, Fudan University, Shanghai 200443, People's Republic of China

^h Also at State Key Laboratory of Nuclear Physics and Technology, Peking University, Beijing 100871, People's Republic of China

ⁱ Also at School of Physics and Electronics, Hunan University, Changsha 410082, China

^j Also at Guangdong Provincial Key Laboratory of Nuclear Science, Institute of Quantum Matter, South China Normal University, Guangzhou 510006, China

^k Also at MOE Frontiers Science Center for Rare Isotopes, Lanzhou University, Lanzhou 730000, People's Republic of China

^l Also at Lanzhou Center for Theoretical Physics, Lanzhou University, Lanzhou 730000, People's Republic of China

^m Also at Ecole Polytechnique Federale de Lausanne (EPFL), CH-1015 Lausanne, Switzerland

ⁿ Also at Helmholtz Institute Mainz, Staudinger Weg 18, D-55099 Mainz, Germany

^o Also at Hangzhou Institute for Advanced Study, University of Chinese Academy of Sciences, Hangzhou 310024, China

^p Currently at Silesian University in Katowice, Chorzow, 41-500, Poland

^q Also at Applied Nuclear Technology in Geosciences Key Laboratory of Sichuan Province, Chengdu University of Technology, Chengdu 610059, People's Republic of China

PLOTS FOR THE VARIOUS ENERGIES

Figures 5, 6, 7, 8, 9, 10 and 11 show the projections of the 2D simultaneous fit on the M_Λ versus M_{BC} distributions in data at $\sqrt{s}=4.600, 4.612, 4.628, 4.641, 4.661, 4.682$ and 4.699 GeV, respectively.

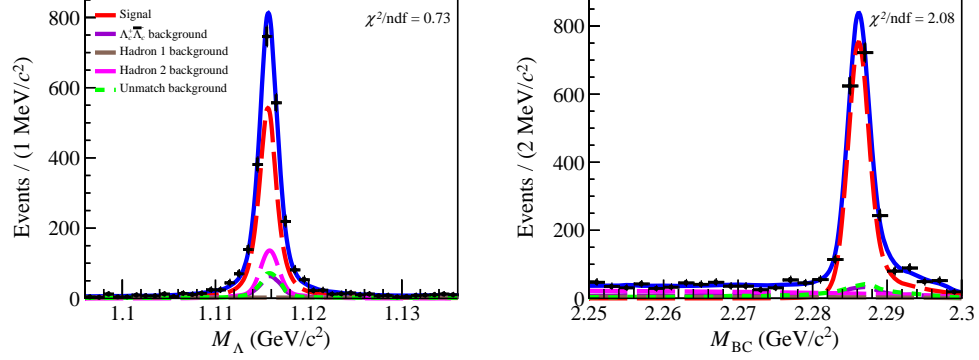


FIG. 5. Projections of the 2D simultaneous fit on the M_Λ versus M_{BC} distributions for the data taken at $\sqrt{s} = 4.600$ GeV. Points with error bars are data, the blue solid lines are the sum of fitting functions, the red dashed lines are the $\Lambda_c^+ \rightarrow \Lambda X$ signal, the purple dashed lines are the $\Lambda_c^+ \bar{\Lambda}_c^-$ background, the brown dashed lines are the “hadron 1” background, the magenta dashed lines are the “hadron 2” background and the green dashed lines are the unmatched background.

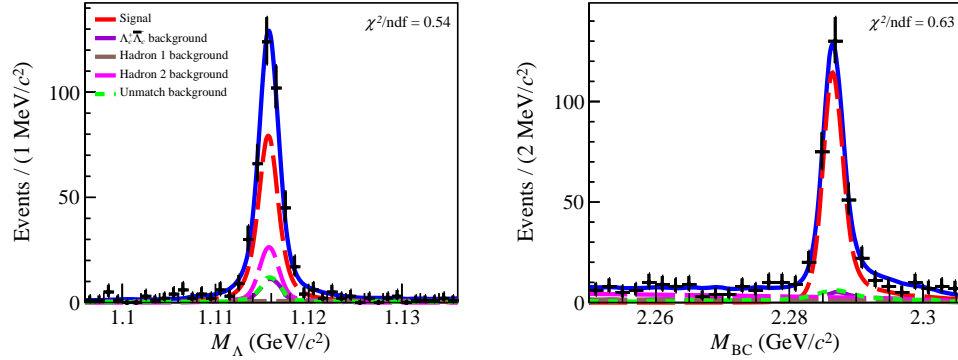


FIG. 6. Projections of the 2D simultaneous fit on the M_Λ versus M_{BC} distributions for the data taken at $\sqrt{s} = 4.612$ GeV. Points with error bars are data, the blue solid lines are the sum of fitting functions, the red dashed lines are the $\Lambda_c^+ \rightarrow \Lambda X$ signal, the purple dashed lines are the $\Lambda_c^+ \bar{\Lambda}_c^-$ background, the brown dashed lines are the “hadron 1” background, the magenta dashed lines are the “hadron 2” background and the green dashed lines are the unmatched background.

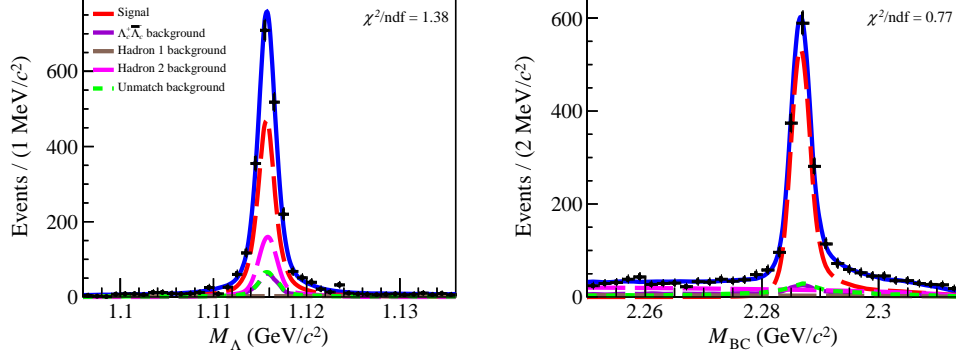


FIG. 7. Projections of the 2D simultaneous fit on the M_Λ versus M_{BC} distributions for the data taken at $\sqrt{s} = 4.628$ GeV. Points with error bars are data, the blue solid lines are the sum of fitting functions, the red dashed lines are the $\Lambda_c^+ \rightarrow \Lambda X$ signal, the purple dashed lines are the $\Lambda_c^+ \bar{\Lambda}_c^-$ background, the brown dashed lines are the “hadron 1” background, the magenta dashed lines are the “hadron 2” background and the green dashed lines are the unmatched background.

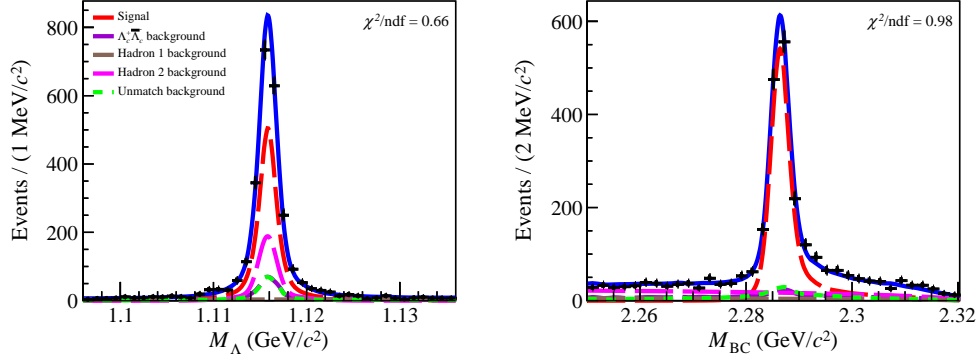


FIG. 8. Projections of the 2D simultaneous fit on the M_Λ versus M_{BC} distributions for the data taken at $\sqrt{s} = 4.641$ GeV. Points with error bars are data, the blue solid lines are the sum of fitting functions, the red dashed lines are the $\Lambda_c^+ \rightarrow \Lambda X$ signal, the purple dashed lines are the $\Lambda_c^+ \bar{\Lambda}_c^-$ background, the brown dashed lines are the “hadron 1” background, the magenta dashed lines are the “hadron 2” background and the green dashed lines are the unmatched background.

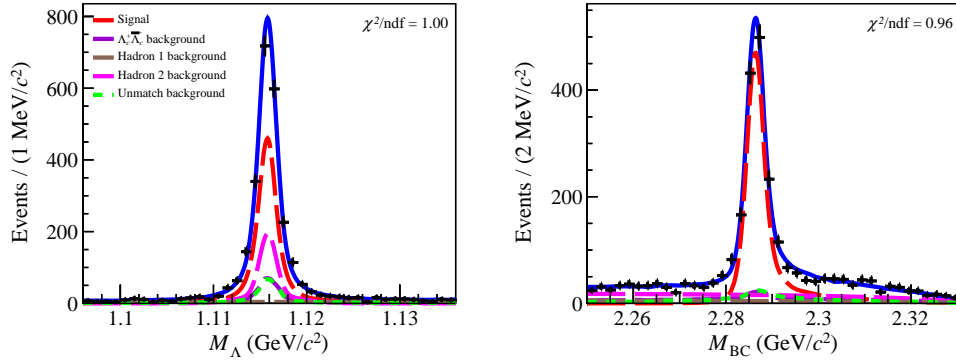


FIG. 9. Projections of the 2D simultaneous fit on the M_Λ versus M_{BC} distributions for the data taken at $\sqrt{s} = 4.661$ GeV. Points with error bars are data, the blue solid lines are the sum of fitting functions, the red dashed lines are the $\Lambda_c^+ \rightarrow \Lambda X$ signal, the purple dashed lines are the $\Lambda_c^+ \bar{\Lambda}_c^-$ background, the brown dashed lines are the “hadron 1” background, the magenta dashed lines are the “hadron 2” background and the green dashed lines are the unmatched background.

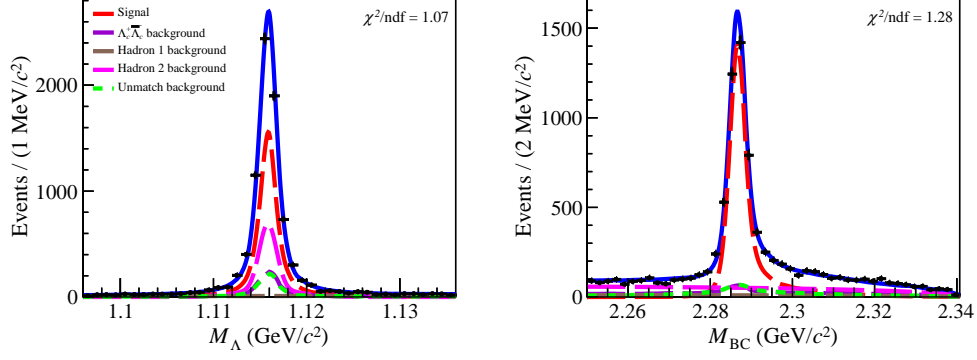


FIG. 10. Projections of the 2D simultaneous fit on the M_Λ versus M_{BC} distributions for the data taken at $\sqrt{s} = 4.682$ GeV. Points with error bars are data, the blue solid lines are the sum of fitting functions, the red dashed lines are the $\Lambda_c^+ \rightarrow \Lambda X$ signal, the purple dashed lines are the $\Lambda_c^+ \bar{\Lambda}_c^-$ background, the brown dashed lines are the “hadron 1” background, the magenta dashed lines are the “hadron 2” background and the green dashed lines are the unmatched background.

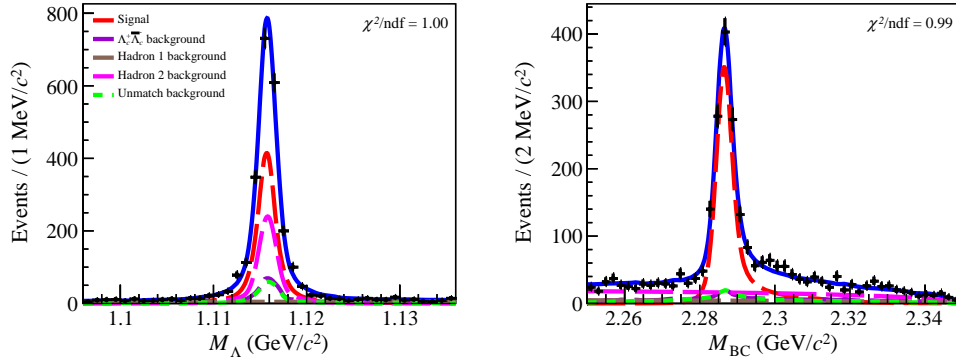


FIG. 11. Projections of the 2D simultaneous fit on the M_Λ versus M_{BC} distributions for the data taken at $\sqrt{s} = 4.699$ GeV. Points with error bars are data, the blue solid lines are the sum of fitting functions, the red dashed lines are the $\Lambda_c^+ \rightarrow \Lambda X$ signal, the purple dashed lines are the $\Lambda_c^+ \bar{\Lambda}_c^-$ background, the brown dashed lines are the “hadron 1” background, the magenta dashed lines are the “hadron 2” background and the green dashed lines are the unmatched background.

PLOTS FOR THE Λ RECOIL INVARIANT MASS SQUARED DISTRIBUTION

Figure 12 shows the Λ recoil invariant mass squared distribution of the weighted data sample. A clear peak near zero is visible, corresponding to the $\Lambda_c^+ \rightarrow \Lambda\pi^+$ decay.

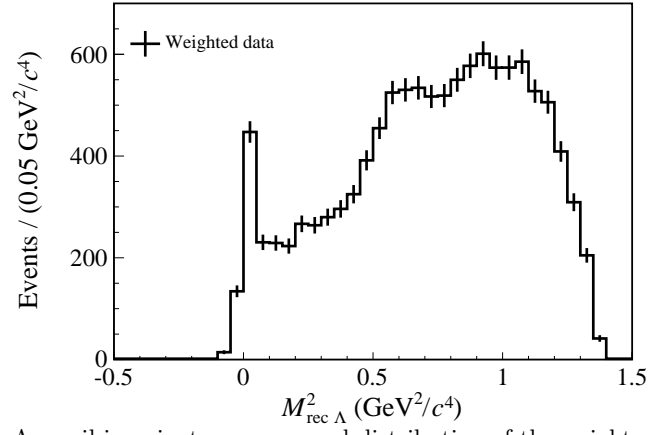


FIG. 12. The Λ recoil invariant mass squared distribution of the weighted data sample.

SYSTEMATIC UNCERTAINTY

Most systematic uncertainties from the ST side cancel out in the determination of the BFs, while those originating from the signal side may introduce systematic biases. The systematic uncertainty due to the Λ reconstruction is taken from the uncertainty of the efficiency correction factor, estimated to be 0.6% using the control samples $J/\psi \rightarrow \bar{p}K^+\Lambda$ and $J/\psi \rightarrow \Lambda\bar{\Lambda}$. Additionally, the systematic uncertainty associated with the intermediate BF of $\Lambda \rightarrow p\pi^-$ is 0.8% [11]. By varying the signal shape, the background shape and the ratio of the size of signal and $\Lambda_c^+\bar{\Lambda}_c^-$ background, the systematic uncertainty related to the 2D fit is evaluated to be 0.4%. The systematic uncertainty in the total ST $\bar{\Lambda}_c^-$ yield is 0.4%, which arises from the fluctuation of signal and background shapes as well as the fit range in the M_{BC} fit. To evaluate the systematic uncertainty from the BDT reweighting procedure, the BDT hyperparameters are varied, with the number of trees changed by $\pm 10\%$ and the maximum tree depth by $\pm 15\%$, yielding an uncertainty of 0.1% estimated from the resulting efficiency differences between the nominal and modified samples. Limited MC statistics contribute an additional uncertainty of 0.2%, quantified through sample size fluctuations. For the unmatched background, an uncertainty of 0.6% is assigned based on the deviation observed in the BF when relaxing the matching angle requirement. Then, the total uncertainty is considered as the quadratic sum of the individual values, corresponding to 1.3%.

The systematic uncertainties arising from imperfect simulation, as well as those associated with the measurement method, can lead to deviations in the measurement of the longitudinal polarization of Λ hyperon. Relevant sources of these uncertainties are summarized in Table I and discussed in the following text. The systematic uncertainty from the Λ reconstruction is also studied with the control samples $J/\psi \rightarrow \bar{p}K^+\Lambda$ and $J/\psi \rightarrow \Lambda\bar{\Lambda}$. Correction factors obtained from these control samples are applied to the signal MC sample, leading to new integration and subsequently new fitting parameters. The systematic uncertainty for the M_{BC} and M_Λ signal regions is evaluated by smearing the signal MC samples using the Gaussian resolution parameters, to account for the resolution differences between data and MC simulation. For the background subtraction, we take into account the background shape and size. The systematic uncertainty associated with the background shape is evaluated by replacing the data sideband sample with the background MC sample from the signal region. To assess the impact of the background size, the fits are repeated using alternative background yields derived from Gaussian sampling of the 2D fit parameters. By sampling the fit parameters under the assumption of a Gaussian distribution, we estimate the systematic uncertainty associated with the background size. The uncertainty is evaluated by combining the fitted Gaussian width and shift of the fitted Gaussian mean from the nominal value. In addition, to account for potential mismodeling of the unmatched background component, an alternative signal MC sample is generated using polarization shifted by one statistical standard deviation from their nominal values, and the resulting variation is assigned as the corresponding systematic uncertainty. The uncertainty from the input parameters of $\alpha_- (\alpha_+)$ is estimated by Gaussian sampling considering their uncertainties. The systematic uncertainty of the MC model is obtained by changing the reweighted hyperparameters. All systematic uncertainties are added in quadrature to calculate the total systematic uncertainties.

TABLE I. The absolute systematic uncertainties (in percent) for the measured longitudinal polarization of Λ hyperon.

Source	\mathcal{P}	$\bar{\mathcal{P}}$
Λ reconstruction	1.8	1.5
Signal region	0.1	0.1
Signal model	0.2	0.1
Background size	0.6	0.4
Background shape	0.1	0.7
Unmatched background model	0.4	0.3
Input parameters	0.4	0.2
Total	2.0	1.7

RESULTS FOR THE YIELDS AND EFFICIENCIES

Table II shows the DT efficiencies for each tag mode at different energy points, where the efficiencies are the overall values including both Λ_c^+ and $\bar{\Lambda}_c^-$ decays.

Tables III, IV, and V show the ST yields, ST and DT efficiencies for each Λ_c^+ tag mode at different energy points, respectively.

Tables VI, VII, and VIII show the ST yields, ST and DT efficiencies for each $\bar{\Lambda}_c^-$ tag mode at different energy points, respectively.

TABLE II. The combined DT efficiencies $\varepsilon_{i,j}^{\text{DT}}$ for each tag mode at different energy points, where the uncertainties are statistical only.

$\varepsilon_{i,j}^{\text{DT}}(\%)$	4.600 GeV	4.612 GeV	4.628 GeV	4.641 GeV	4.661 GeV	4.682 GeV	4.699 GeV
$\bar{p}K_S^0$	22.9 ± 0.3	21.4 ± 0.7	20.4 ± 0.3	20.2 ± 0.3	20.0 ± 0.3	20.0 ± 0.2	18.3 ± 0.3
$\bar{p}K^+\pi^-$	20.5 ± 0.1	19.1 ± 0.3	20.1 ± 0.1	18.5 ± 0.1	18.9 ± 0.1	19.0 ± 0.1	17.9 ± 0.1
$\bar{p}K_S^0\pi^0$	8.4 ± 0.2	7.9 ± 0.4	7.8 ± 0.2	7.5 ± 0.2	7.6 ± 0.2	7.6 ± 0.1	7.0 ± 0.2
$\bar{p}K_S^0\pi^-\pi^+$	8.2 ± 0.2	7.1 ± 0.4	7.2 ± 0.2	7.2 ± 0.2	7.2 ± 0.2	7.2 ± 0.1	6.8 ± 0.2
$\bar{p}K^+\pi^-\pi^0$	6.5 ± 0.1	5.8 ± 0.2	6.0 ± 0.1	5.7 ± 0.1	5.9 ± 0.1	6.1 ± 0.1	5.8 ± 0.1
$\bar{\Lambda}\pi^-$	19.4 ± 0.2	17.8 ± 0.5	17.1 ± 0.2	16.3 ± 0.2	16.7 ± 0.2	15.5 ± 0.1	15.2 ± 0.2
$\bar{\Lambda}\pi^-\pi^0$	10.6 ± 0.1	9.8 ± 0.2	9.8 ± 0.1	9.2 ± 0.1	9.4 ± 0.1	9.3 ± 0.1	8.7 ± 0.1
$\bar{\Lambda}\pi^-\pi^+\pi^-$	7.4 ± 0.1	6.9 ± 0.2	7.0 ± 0.1	6.4 ± 0.1	6.8 ± 0.1	7.1 ± 0.1	6.5 ± 0.1
$\bar{\Sigma}^0\pi^-$	12.9 ± 0.2	11.9 ± 0.5	11.9 ± 0.2	11.5 ± 0.2	11.0 ± 0.2	11.3 ± 0.1	10.7 ± 0.2
$\bar{\Sigma}^-\pi^0$	8.6 ± 0.3	8.4 ± 0.6	8.6 ± 0.3	8.5 ± 0.3	8.1 ± 0.3	8.2 ± 0.2	7.7 ± 0.3
$\bar{\Sigma}^-\pi^-\pi^+$	9.0 ± 0.1	8.8 ± 0.3	8.8 ± 0.1	8.2 ± 0.1	8.2 ± 0.1	8.3 ± 0.1	7.5 ± 0.1

TABLE III. The ST yields $N_{i,j}^{\text{ST}}$ for each Λ_c^+ tag mode at different energy points, where the uncertainties are statistical only.

$\Lambda_c^+ \rightarrow \text{tag modes}$	4.600 GeV	4.612 GeV	4.628 GeV	4.641 GeV	4.661 GeV	4.682 GeV	4.699 GeV
pK_S^0	645 ± 26	113 ± 11	515 ± 24	557 ± 25	537 ± 24	1645 ± 43	458 ± 23
$pK^-\pi^+$	3295 ± 65	592 ± 28	2909 ± 62	3136 ± 64	3025 ± 62	8572 ± 104	2486 ± 56
$pK_S^0\pi^0$	291 ± 24	65 ± 12	300 ± 28	288 ± 26	290 ± 27	870 ± 46	224 ± 25
$pK_S^0\pi^+\pi^-$	321 ± 26	46 ± 11	261 ± 25	252 ± 24	297 ± 25	760 ± 42	232 ± 24
$pK^-\pi^+\pi^0$	964 ± 53	165 ± 23	840 ± 50	744 ± 51	729 ± 50	2392 ± 92	672 ± 52
$\Lambda\pi^+$	377 ± 20	64 ± 8	330 ± 20	360 ± 20	327 ± 19	1049 ± 34	259 ± 17
$\Lambda\pi^+\pi^0$	858 ± 40	146 ± 16	750 ± 37	823 ± 40	727 ± 36	2204 ± 63	636 ± 35
$\Lambda\pi^+\pi^-\pi^+$	418 ± 27	80 ± 12	297 ± 24	375 ± 26	428 ± 33	1040 ± 45	321 ± 25
$\Sigma^0\pi^+$	250 ± 18	53 ± 8	171 ± 15	211 ± 17	223 ± 17	733 ± 30	175 ± 15
$\Sigma^+\pi^0$	167 ± 18	43 ± 11	149 ± 17	152 ± 18	131 ± 17	456 ± 32	120 ± 17
$\Sigma^+\pi^+\pi^-$	587 ± 34	125 ± 17	438 ± 32	560 ± 36	495 ± 34	1515 ± 62	479 ± 37

TABLE IV. The ST efficiencies $\varepsilon_{i,j}^{\text{ST}}(\%)$ for each Λ_c^+ tag mode at different energy points, where the uncertainties are statistical only.

$\Lambda_c^+ \rightarrow \text{tag modes}$	4.600 GeV	4.612 GeV	4.628 GeV	4.641 GeV	4.661 GeV	4.682 GeV	4.699 GeV
pK_S^0	56.1 ± 0.3	53.4 ± 0.8	51.8 ± 0.3	50.7 ± 0.3	49.7 ± 0.3	48.6 ± 0.2	47.6 ± 0.3
$pK^-\pi^+$	51.5 ± 0.1	51.2 ± 0.3	49.4 ± 0.1	49.1 ± 0.1	48.4 ± 0.1	47.5 ± 0.1	47.0 ± 0.1
$pK_S^0\pi^0$	22.7 ± 0.2	23.0 ± 0.6	20.9 ± 0.2	20.8 ± 0.2	19.7 ± 0.2	19.2 ± 0.1	18.6 ± 0.2
$pK_S^0\pi^+\pi^-$	24.0 ± 0.3	21.5 ± 0.6	21.5 ± 0.3	21.8 ± 0.3	21.4 ± 0.3	22.0 ± 0.2	19.4 ± 0.3
$pK^-\pi^+\pi^0$	19.3 ± 0.1	19.8 ± 0.3	18.2 ± 0.1	17.2 ± 0.1	17.7 ± 0.1	17.1 ± 0.1	17.3 ± 0.1
$\Lambda\pi^+$	47.6 ± 0.4	45.5 ± 0.9	41.6 ± 0.4	40.5 ± 0.4	40.1 ± 0.4	40.1 ± 0.2	37.9 ± 0.4
$\Lambda\pi^+\pi^0$	20.8 ± 0.1	18.9 ± 0.3	18.5 ± 0.1	18.6 ± 0.1	18.4 ± 0.1	17.6 ± 0.1	17.5 ± 0.1
$\Lambda\pi^+\pi^-\pi^+$	16.0 ± 0.2	13.7 ± 0.4	14.1 ± 0.2	14.4 ± 0.2	14.2 ± 0.2	14.2 ± 0.1	14.8 ± 0.2
$\Sigma^0\pi^+$	28.0 ± 0.3	24.5 ± 0.8	25.8 ± 0.3	25.2 ± 0.3	25.4 ± 0.3	24.7 ± 0.2	23.4 ± 0.3
$\Sigma^+\pi^0$	22.8 ± 0.4	21.5 ± 0.8	22.4 ± 0.4	24.9 ± 0.4	22.4 ± 0.4	22.2 ± 0.2	21.4 ± 0.4
$\Sigma^+\pi^+\pi^-$	25.1 ± 0.2	25.2 ± 0.5	23.2 ± 0.2	22.8 ± 0.2	22.9 ± 0.2	22.3 ± 0.1	22.1 ± 0.2

TABLE V. The DT efficiencies $\varepsilon_{i,j}^{\text{DT}}(\%)$ for each Λ_c^+ tag mode at different energy points, where the uncertainties are statistical only.

$\Lambda_c^+ \rightarrow \text{tag modes}$	4.600 GeV	4.612 GeV	4.628 GeV	4.641 GeV	4.661 GeV	4.682 GeV	4.699 GeV
pK_S^0	22.2 ± 0.4	19.7 ± 0.9	20.5 ± 0.4	20.1 ± 0.4	19.5 ± 0.4	19.7 ± 0.2	18.0 ± 0.4
$pK^-\pi^+$	20.1 ± 0.2	19.6 ± 0.4	20.1 ± 0.2	18.4 ± 0.2	18.8 ± 0.2	19.0 ± 0.1	17.9 ± 0.2
$pK_S^0\pi^0$	8.0 ± 0.2	8.1 ± 0.5	7.7 ± 0.2	7.4 ± 0.2	7.3 ± 0.2	7.8 ± 0.1	7.2 ± 0.2
$pK_S^0\pi^+\pi^-$	7.9 ± 0.3	7.2 ± 0.6	7.6 ± 0.3	7.8 ± 0.3	7.4 ± 0.3	7.2 ± 0.1	6.8 ± 0.3
$pK^-\pi^+\pi^0$	6.4 ± 0.1	6.2 ± 0.3	6.0 ± 0.1	5.8 ± 0.1	6.0 ± 0.1	6.0 ± 0.1	5.8 ± 0.1
$\Lambda\pi^+$	18.5 ± 0.3	17.5 ± 0.7	16.2 ± 0.3	15.5 ± 0.3	15.9 ± 0.3	14.9 ± 0.2	14.3 ± 0.3
$\Lambda\pi^+\pi^0$	10.8 ± 0.1	9.8 ± 0.2	9.8 ± 0.1	9.1 ± 0.1	9.3 ± 0.1	9.1 ± 0.1	8.7 ± 0.1
$\Lambda\pi^+\pi^-\pi^+$	7.6 ± 0.1	7.0 ± 0.2	7.1 ± 0.1	6.5 ± 0.1	7.0 ± 0.1	7.3 ± 0.1	6.5 ± 0.1
$\Sigma^0\pi^+$	12.8 ± 0.3	9.7 ± 0.6	11.4 ± 0.3	11.1 ± 0.3	10.6 ± 0.3	11.1 ± 0.2	10.3 ± 0.3
$\Sigma^+\pi^0$	8.1 ± 0.4	8.6 ± 0.8	8.2 ± 0.4	8.2 ± 0.4	8.1 ± 0.4	8.2 ± 0.2	7.7 ± 0.4
$\Sigma^+\pi^+\pi^-$	9.0 ± 0.2	8.7 ± 0.4	8.8 ± 0.2	8.3 ± 0.2	8.3 ± 0.2	8.3 ± 0.1	7.4 ± 0.2

TABLE VI. The ST yields $N_{i,j}^{\text{ST}}$ for each $\bar{\Lambda}_c^-$ tag mode at different energy points, where the uncertainties are statistical only.

$\bar{\Lambda}_c^- \rightarrow \text{tag modes}$	4.600 GeV	4.612 GeV	4.628 GeV	4.641 GeV	4.661 GeV	4.682 GeV	4.699 GeV
$\bar{p}K_S^0$	633 ± 26	126 ± 12	540 ± 25	552 ± 25	582 ± 25	1734 ± 44	501 ± 24
$\bar{p}K^+\pi^-$	3516 ± 64	576 ± 27	2992 ± 62	3125 ± 63	2924 ± 60	8970 ± 104	2699 ± 57
$\bar{p}K_S^0\pi^0$	318 ± 24	62 ± 11	296 ± 24	315 ± 25	298 ± 24	922 ± 43	245 ± 23
$\bar{p}K_S^0\pi^-\pi^+$	292 ± 23	60 ± 11	235 ± 21	276 ± 22	260 ± 22	788 ± 38	234 ± 21
$\bar{p}K^+\pi^-\pi^0$	1193 ± 55	192 ± 22	748 ± 47	973 ± 52	1002 ± 53	2664 ± 88	713 ± 48
$\bar{\Lambda}\pi^-$	380 ± 20	56 ± 8	346 ± 20	345 ± 20	344 ± 20	1028 ± 34	280 ± 18
$\bar{\Lambda}\pi^-\pi^0$	888 ± 39	164 ± 17	730 ± 36	798 ± 37	770 ± 36	2202 ± 61	685 ± 34
$\bar{\Lambda}\pi^-\pi^+\pi^-$	355 ± 24	58 ± 10	291 ± 22	374 ± 25	349 ± 24	1048 ± 42	330 ± 24
$\bar{\Sigma}^0\pi^-$	276 ± 19	49 ± 8	243 ± 16	237 ± 18	233 ± 18	670 ± 29	197 ± 16
$\bar{\Sigma}^-\pi^0$	149 ± 17	31 ± 7	119 ± 16	143 ± 17	168 ± 18	432 ± 30	132 ± 17
$\bar{\Sigma}^-\pi^-\pi^+$	621 ± 39	95 ± 15	561 ± 33	520 ± 34	558 ± 34	1616 ± 60	480 ± 33

TABLE VII. The ST efficiencies $\varepsilon_{i,j}^{\text{ST}}(\%)$ for each $\bar{\Lambda}_c^-$ tag mode at different energy points, where the uncertainties are statistical only.

$\bar{\Lambda}_c^- \rightarrow \text{tag modes}$	4.600 GeV	4.612 GeV	4.628 GeV	4.641 GeV	4.661 GeV	4.682 GeV	4.699 GeV
$\bar{p}K_S^0$	56.3 ± 0.3	54.0 ± 0.8	51.8 ± 0.3	50.9 ± 0.3	49.6 ± 0.3	48.7 ± 0.2	47.6 ± 0.3
$\bar{p}K^+\pi^-$	51.4 ± 0.1	51.0 ± 0.3	49.2 ± 0.1	48.2 ± 0.1	48.2 ± 0.1	46.8 ± 0.1	45.7 ± 0.1
$\bar{p}K_S^0\pi^0$	23.3 ± 0.2	21.6 ± 0.6	20.8 ± 0.2	20.9 ± 0.2	20.7 ± 0.2	20.4 ± 0.1	19.5 ± 0.2
$\bar{p}K_S^0\pi^-\pi^+$	23.1 ± 0.3	22.2 ± 0.6	19.9 ± 0.3	20.1 ± 0.3	20.8 ± 0.3	19.6 ± 0.2	19.8 ± 0.3
$\bar{p}K^+\pi^-\pi^0$	22.2 ± 0.1	20.7 ± 0.3	19.5 ± 0.1	19.6 ± 0.1	19.1 ± 0.1	18.9 ± 0.1	18.2 ± 0.1
$\bar{\Lambda}\pi^-$	49.2 ± 0.4	48.4 ± 0.9	44.6 ± 0.4	45.2 ± 0.4	43.3 ± 0.4	42.6 ± 0.2	40.8 ± 0.4
$\bar{\Lambda}\pi^-\pi^0$	21.8 ± 0.1	20.7 ± 0.3	19.8 ± 0.1	19.6 ± 0.1	19.4 ± 0.1	18.8 ± 0.1	18.5 ± 0.1
$\bar{\Lambda}\pi^-\pi^+\pi^-$	15.3 ± 0.2	13.5 ± 0.4	13.7 ± 0.2	14.1 ± 0.2	14.0 ± 0.2	13.8 ± 0.1	14.5 ± 0.2
$\bar{\Sigma}^0\pi^-$	30.9 ± 0.4	28.9 ± 0.8	28.7 ± 0.4	27.1 ± 0.3	27.6 ± 0.4	27.2 ± 0.2	25.3 ± 0.4
$\bar{\Sigma}^-\pi^0$	24.5 ± 0.4	23.6 ± 0.9	24.5 ± 0.4	24.8 ± 0.4	24.0 ± 0.4	23.1 ± 0.2	23.0 ± 0.4
$\bar{\Sigma}^-\pi^-\pi^+$	25.8 ± 0.2	26.3 ± 0.5	23.7 ± 0.2	23.9 ± 0.2	23.4 ± 0.2	22.4 ± 0.1	22.9 ± 0.2

TABLE VIII. The DT efficiencies $\varepsilon_{i,j}^{\text{DT}}(\%)$ for each $\bar{\Lambda}_c^-$ tag mode at different energy points, where the uncertainties are statistical only.

$\bar{\Lambda}_c^- \rightarrow \text{tag modes}$	4.600 GeV	4.612 GeV	4.628 GeV	4.641 GeV	4.661 GeV	4.682 GeV	4.699 GeV
$\bar{p}K_S^0$	23.7 ± 0.4	22.9 ± 0.9	20.3 ± 0.4	20.4 ± 0.4	20.4 ± 0.4	20.2 ± 0.2	18.7 ± 0.4
$\bar{p}K^+\pi^-$	21.1 ± 0.2	18.7 ± 0.4	20.2 ± 0.2	18.6 ± 0.2	19.1 ± 0.2	19.1 ± 0.1	18.0 ± 0.2
$\bar{p}K_S^0\pi^0$	8.8 ± 0.3	7.7 ± 0.5	7.9 ± 0.3	7.7 ± 0.2	7.9 ± 0.3	7.4 ± 0.1	6.8 ± 0.2
$\bar{p}K_S^0\pi^-\pi^+$	8.4 ± 0.3	7.1 ± 0.6	6.7 ± 0.3	6.5 ± 0.2	6.9 ± 0.3	7.2 ± 0.2	6.8 ± 0.3
$\bar{p}K^+\pi^-\pi^0$	6.6 ± 0.1	5.4 ± 0.3	6.0 ± 0.1	5.6 ± 0.1	5.7 ± 0.1	6.1 ± 0.1	5.7 ± 0.1
$\bar{\Lambda}\pi^-$	20.4 ± 0.4	18.0 ± 0.7	18.0 ± 0.3	17.1 ± 0.3	17.6 ± 0.3	16.1 ± 0.2	16.1 ± 0.3
$\bar{\Lambda}\pi^-\pi^0$	10.4 ± 0.1	9.9 ± 0.2	10.0 ± 0.1	9.3 ± 0.1	9.5 ± 0.1	9.4 ± 0.1	8.7 ± 0.1
$\bar{\Lambda}\pi^-\pi^+\pi^-$	7.2 ± 0.1	6.7 ± 0.3	6.8 ± 0.1	6.3 ± 0.1	6.5 ± 0.1	6.9 ± 0.1	6.5 ± 0.1
$\bar{\Sigma}^0\pi^-$	13.1 ± 0.3	14.2 ± 0.7	12.5 ± 0.3	11.9 ± 0.3	11.4 ± 0.3	11.6 ± 0.2	11.2 ± 0.3
$\bar{\Sigma}^-\pi^0$	9.2 ± 0.4	8.2 ± 0.8	9.0 ± 0.4	8.8 ± 0.4	8.1 ± 0.4	8.2 ± 0.2	7.8 ± 0.4
$\bar{\Sigma}^-\pi^-\pi^+$	9.1 ± 0.2	8.9 ± 0.4	8.9 ± 0.2	8.1 ± 0.2	8.2 ± 0.2	8.3 ± 0.1	7.7 ± 0.2